

Published in final edited form as:

Nat Chem Biol. 2024 November; 20(11): 1482–1492. doi:10.1038/s41589-024-01665-7.

Simultaneous multi-site editing of individual genomes using retron arrays

Alejandro González-Delgado $^{1,\#}$, Santiago C. Lopez $^{1,2,\#}$, Matías Rojas-Montero 1 , Chloe B. Fishman 1 , Seth L. Shipman 1,3,4,*

¹Gladstone Institute of Data Science and Biotechnology, San Francisco, CA, USA

²Graduate Program in Bioengineering, University of California, San Francisco and Berkeley, CA, USA

³Department of Bioengineering and Therapeutic Sciences, University of California, San Francisco, CA, USA

⁴Chan Zuckerberg Biohub – San Francisco, San Francisco, CA

Abstract

During recent years the use of libraries-scale genomic manipulations scaffolded on CRISPR gRNAs have been transformative. However, these existing approaches are typically multiplexed across genomes. Unfortunately, building cells with multiple, non-adjacent precise mutations remains a laborious cycle of editing, isolating an edited cell, and editing again. The use of bacterial retrons can overcome this limitation. Retrons are genetic systems composed of a reverse transcriptase and a non-coding RNA (ncRNA) that contains an msd, which is reverse transcribed to produce multiple copies of single-stranded DNA. Here, we describe a technology – termed a multitron – for precisely modifying multiple sites on a single genome simultaneously using retron arrays, in which multiple donor-encoding DNAs are produced from a single transcript. The multitron architecture is compatible with both recombineering in prokaryotic cells and CRISPR editing in eukaryotic cells. We demonstrate applications for this approach in molecular recording, genetic element minimization, and metabolic engineering.

INTRODUCTION

Multiplexing – the act of consolidating multiple discrete elements into a single composite channel – has enabled genomic technologies to scale toward the complexity of the biology we hope to understand. Today, one might use multiplexed DNA synthesis to make a library

#equal contributions

Author Contributions

S.L.S., A.G.-D. and S.C.L. conceived the study. A.G.-D., S.C.L., M.R.M. and C.B.F. performed the experiments; A.G.-D., S.C.L. and S.L.S. designed the work, analyzed the data and wrote the manuscript.

Competing Interests

A.G.-D., S.C.L., and S.L.S. are named inventors on a patent application related to the technologies described in this work. S.L.S. is a founder of Retronix Bio. 'The remaining authors declare no competing interests.

Code Availability

Custom code to process or analyze data from this study is available on GitHub: https://github.com/Shipman-Lab/multitrons

^{*}Correspondence to: seth.shipman@gladstone.ucsf.edu.

of distinct CRISPR gRNAs on a single synthesis chip, then use multiplexed experimental design to clone and transfect that library of gRNAs across cells in a single culture, and finally use multiplexed sequencing to analyze the effect of the perturbation on a single sequencing flow-cell^{1,2}. This now-standard multiplexed gRNA workflow has allowed scientists run experiments across every gene in parallel with barely more effort than they might have previously put into determining the effect of single gene. However, the typical multiplexing of a gRNA library precludes an important level of analysis: it is implemented across cells, where a single edit is made per genome, and thus cannot be used to study the interaction of mutations within a genome.

Technologies for multiplexing *within* genomes – where multiple distinct, non-adjacent edits are made using a single, consolidated editor – are much more limited. Yet, applications for multiplexing within genomes abound in both fundamental biology (e.g. studying epistasis, long-range gene regulation, and genome organization) and biotechnology (e.g. metabolic engineering, molecular recording, and genome minimization). These complex applications require precise mutations, not genomic scars or transcriptional perturbations. Precision is essential to understand combinatorial genome complexity, such as probing compensatory mutations across genes in a complex or interrogating enhancer-promoter interactions, and is necessary to build nuanced technological advances, such as ribosome-dependent tuning of gene expression in a metabolic pathway.

In bacteria, the most commonly used approach to introduce combinatorial, precise mutations is MAGE (multiplexed automated genome engineering), which relies on single stranded DNA (ssDNA) recombineering^{3–5}. A eukaryotic version of this technology has been developed to extend this approach to yeast⁶. However, MAGE is limited by its requirement for numerous labor-intensive recombineering cycles required to attain efficient combinatorial editing rates, and by its reliance on exogenously-delivered oligonucleotides that leave no trackable plasmid element for phenotyping by proxy⁷. Base-editing (BE) and prime-editing (PE)^{8–10} are two other precise editing approaches that can be multiplexed^{11–16}. Base-editors are the simplest to multiplex using tandem gRNAs, but are limited to single base mutations of a defined type (either A•T-to-G•C or C•G-to-T•A)^{11,13–14}. Prime-editors have also been multiplexed, but the complexity of the editing elements grows quickly with additional sites. In bacteria, multiplexed prime editing requires a three plasmid system, and multiple edits occur on the same genome in less than 1% of cells¹², while systems built for human and plant cells require two gRNAs per site in addition to the editing template, which can create issues with the assembly of multiplexed plasmids^{14–16}.

Another way to introduce precise mutations that is compatible with both prokaryotic and eukaryotic editing is to produce editing donors inside a cell using modified retrons. Retrons are bacterial tripartite systems that have been shown to provide phage defense^{17–20}. Two of the components of the retron operon are a reverse transcriptase and a small (200–300 base), structured non-coding RNA (ncRNA). The reverse transcriptase recognizes and partially reverse transcribes the ncRNA into a single-stranded DNA fragment that is present at the abundance of a cellular transcript^{18,21–24}.

We and others have previously shown that the retron ncRNA can be modified to encode an editing donor to precisely edit the genomes of bacteria, phage, plant, yeast, and even human cells^{25–31}. However, these retron-derived editors have only been used to edit genomic positions one at a time. Here, we describe a substantial modification of the retron ncRNA to produce multiple editing donors simultaneously from a single transcript after reverse transcription. We show that these multiplexed, arrayed retron elements – termed multitrons – can be paired with single-stranded annealing proteins to edit prokaryotic genomes and with CRISPR components to edit eukaryotic genomes^{26–29}. We demonstrate utility with proof-of-concept applications in molecular recording, multiplexed deletions, and metabolic engineering.

RESULTS

Multiplexed editing from multiple donors in a retron msd

The use of retrons in bacterial recombineering was originally developed for applications in molecular recording²⁵, and has more recently been optimized to install single targeted edits and interrogate biology^{26–29}. To do so, a retron ncRNA – which can be divided into two regions: an msr (multicopy single-stranded RNA) that is not reverse transcribed and an msd (multicopy single-stranded DNA) that is reverse transcribed – is modified to encode an editing donor within the msd region. This modified ncRNA is expressed in cells along with a retron reverse transcriptase (e.g. retron Eco1-RT) that reverse transcribes the retron msd to produce an editing donor (RT-Donor). An overexpressed single-stranded annealing protein (SSAP, e.g. CspRecT) and the host single-stranded binding protein (SSB) promote annealing of the RT-Donor to the lagging strand of a replicating chromosome to install the edited sequence^{32–33}.

We aimed to further modify retrons to create multitron editors, capable of multiplexed editing of a single genome from a consolidated retron element generating multiple RT-Donors per transcript. Recombineering via oligonucleotide donors is most efficient with donors between 70 and 90 bases long³, which is also the ideal range for retron recombineering donors^{28,31}. Yet, retron RTs are capable of reverse transcribing much longer RT-Donors, even up to an entire gene length²⁶. Thus, we initially tested a multitron architecture that encodes multiple 70 bp donors end-to-end within a single msd loop (Fig 1a) using the two tandem donors to make point mutations in both the *rpoB* and *gyrA* genes in *E. coli*. We tested two versions of this multitron with the donors in each of the possible orders in the msd as well as a control *rpoB* singleplex editor. Both tandem multitron variants edited both sites, and editing rates for *rpoB* were comparable in the singleplex versus multitron configurations (Fig 1b).

When comparing the two multitron versions, we noticed that the site edited by the first donor in the multitron tended to have a higher editing rate than the site edited by the second donor. The donor in position one is reverse transcribed first, so the editing difference could be due to a small effect of RT processivity, or due to a positional effect of the donors after reverse transcription. To distinguish between these possibilities, we compared the relative editing efficiencies at each site using the multitrons versus synthetic oligonucleotides of the same sequence as the tandem RT-Donors. Unlike RT-Donors produced by multitrons,

oligonucleotide donors had similar relative editing rates across the sites independent of their donor position (Fig 1c), consistent with an effect of RT processivity.

We next tested three donor multitrons in the tandem msd architecture, using a third donor targeting lacZ on the leading strand (less effective than targeting the lagging strand). All three sites were edited in each of the three permutations of donor order (Fig 1d), with the same positional bias for higher editing at the 5' end of the RT-Donor (Fig 1e). Although the positional bias is a bug in our intended design, we wondered whether it could be exploited to create a range of editing efficiencies for analog molecular recording. Retrons have previously been used as analog molecular recorders capable of detecting the magnitude and duration of a specific input by accumulating precise mutations in the genome²⁵. These analog molecular recorders are, however, limited to operating in the linear range of the interaction between reporter and editing efficacy. We reasoned that using a tandem multitron could add robustness by expanding the dynamic range of a recording across multiple sites. We constructed another multitron encoding three lagging donors (gyrA, priB, rpoB) driven by an m-toluic acid (mTol)-inducible promoter. Here too, we found that the editing rates were inversely proportional to the order of donor reverse transcription at maximal induction (Fig 1f). As a result, the editing rates for each site saturate at different mTol concentrations when used as an analog recorder of mTol (Fig 1g), effectively increasing the dynamic range of the recorder.

Improved Multiplexed Editing Using Donors in Retron Arrays

To overcome the effect of donor position inside a single msd loop, we engineered a different version of the multitron architecture composed of an ncRNA array with multiple msr-msd regions in tandem, each one containing a distinct donor to edit a unique target site (Fig 2a). With this arrayed ncRNA multitron, the retron RT has different substrates available within a transcript to generate multiple RT-donors independently, each at the same distance from an internal RT priming site. We tested the ability of this arrayed ncRNA multitron to edit *rpoB* and *gyrA* versus singleplex retron editors, and found that the arrayed ncRNA multitron performed as well or better than the singleplex versions (Fig 2a). However, this arrayed ncRNA created a new constraint. The length of the ncRNA donor unit is 229 bp and the arrayed design adds 109 bp of direct repeat for each additional editor due to msr duplication, both of which pose challenges for the synthesis and assembly of new multitron plasmids.

Therefore, we engineered a third multitron version composed of an msd array rather than an ncRNA array. In this case, each msd encodes a distinct donor as in the previous version, but the msr is expressed in trans as a separate transcript (Fig 2b). This trans msr arrangement was previously shown to be a tolerated modification for reverse transcription of endogenous retron msds³⁴. In practice, this reduces the editing unit to 149 bp and reduces the length of the longest direct repeat to 74 bases. The trans msr can interact with any of the arrayed msds, again keeping the donor at a constant distance from the site of RT priming (Fig 2c).

We tested editing by the arrayed msd multitron versus singleplex editors and found no difference in editing rates at either site (Fig 2b). The trans msr arrangement in fact yielded consistently higher editing rates than the endogenous retron ncRNA architecture in both singleplex and multiplexed forms throughout this project. Although the msd array and

msr/RT transcript contain no terminator between them and could potentially be transcribed as a single unit rather than the intended trans arrangement, we found both sites could be edited at a similar efficiency when using a plasmid containing a terminator between the msd array and the msr (Extended Data Fig. 1).

To test whether donor position inside the msd array multitron affects editing, we constructed three multitron variants with donors to edit *priB*, *rpoB* and *gyrA* genes in each possible order. All three sites were edited by each multitron variant (Fig 2d), and there was no effect of donor position using arrayed msds (Fig 2e). Finally, to push the limits of within-genome multiplexing, we constructed an arrayed msd multitron to simultaneously edit 5 target sites (*hda*, *fbaH*, *priB*, *rpoB* and *gyrA*). Editing rates ranged from 5 to 25% for each site, illustrating that arrayed msd multitrons are a potent tool for multiplexed genome editing technologies (Fig 2f).

Increasing Limits of Deletion Size Using Nested Multitrons

One benefit of using retron-derived donors is that they support a broad range of precise mutations, including insertions, deletions and replacements. However, when recombineering with either retron RT-Donor or oligonucleotide donors, the efficiency of inserting and deleting base pairs is inversely related to the size of the edit^{3,31}. This is presumably intrinsic to the mechanism of recombineering, a result that we replicated here using RT-Donors to delete 1 to 100 bp, finding a declining efficiency with deletion size whether using an endogenous ncRNA architecture or the trans msr architecture (Fig 3a).

We wondered whether we could overcome this limitation on deletion efficiency at larger sizes by using arrayed msd multitrons encoding a series of nested deletion donors. A nested deletion series consists of multiple donors intended to make deletions of increasing size progressively at same locus. If the smallest deletion succeeds, it creates a smaller target size for a previously disfavored large deletion. We explored nested deletions by first comparing the editing efficiency of single 25 and 50 bp deletions in the *lacZ* gene with simultaneous deletions of overlapping 25 and 50 bp at the same location using a multitron (Fig 3b). The 50 bp deletion was not significantly less efficient than the 25 bp deletion using singleplex retron donors so, unsurprisingly, the rate of 50 bp deletions by the multitron version was not significantly increased. However, the rate of the 25 bp deletion was decreased by the multitron, suggesting that 25 bp deletions were being converted into 50 bp deletions.

Next, we tested a multitron containing a 25, 50, and 100 bp nested deletion donor series (Fig 3c). In this case, the previously disfavored 100 bp deletion was significantly more efficient using the multitron series than using the singleplex deletion donor. In fact, this strategy created a 100 bp deletion in ~42% of genomes, overcoming an intrinsic inefficiency in recombineering deletions. Furthermore, the multitrons generated a heterogeneous population of genetic elements with different deletions sizes that could be used to probe functional domains of a target gene or miniature versions of a protein of interest.

Multiple Edits in an Individual Genome Using Multitrons

Up to this point, editing has been quantified by bulk sequencing of each individual locus, with the assumption that edits accumulate on genomes according to the product of the rates

at each site. We next aimed to explicitly test that assumption. First, we designed a multitron editor producing three, non-overlapping msd donors, each targeting a single gene, *gyrA*, in a genome window of 300 bp (Fig 4a). All 70 bp donors target the lagging strand. With this narrow editing window, we were able to analyze recombineering efficiencies for individual sites as well as combinatorial edits from an amplicon of the locus. Sequencing revealed editing rates of 8 to 25% across the sites, comparable to previous experiments (Fig 4a). From this individual site data, we calculated an expected frequency that we should find the various double edits and the triple edits among genomes, based on the product of rates at each site (Fig 4b). We compared this to the real frequency of each double combination and the triple edit in our sequencing data and found that the expected and real rates were matched (Fig 4b). Here, the double edits were present in 1.4–7.1% of genomes and the triple edit was present in ~0.77% of genomes.

To test the accumulation of multiple edits on individual genomes in a more practical scenario, we decided to isolate multiply edited clones using a single editing plasmid that can be easily removed after editing. To do this, we combined the five molecular elements required for multitron recombineering – msd array, msr, RT, RecT, and dominant negative mutL (to suppress mismatch repair for single base mutations) – onto a single plasmid with RSF1010 origin of replication (Extneded Data Fig. 2a). However, initial testing of this architecture yielded editing rates for the *rpoB* gene were ~5x lower using the single plasmid compared to the previous two plasmid system (~5% and ~25%, respectively). To increase recombineering efficiency, we added an *E. coli* optimized ribosome binding site (RBS) immediately upstream of only the RT gene or both the RT and the CspRecT genes, both of which increased editing rates but still fell short of the level achieved by the two-plasmid system (Extended Data Fig. 2a).

We next changed the origin of replication for the single plasmid system, opting for a temperature-sensitive origin (oriR101) so that the plasmid becomes curable after editing by moving from a permissive temperature (30°C) to a non-permissive temperature (37°C)^{35,36}. Interestingly, the editing rates using this single plasmid finally reached comparable levels to those of the previous the two-plasmid system (Extended Data Fig. 2a). This improvement in editing was not due to an effect of temperature, as we found similar editing rates with a temperature-insensitive version at both 30°C and 37°C (Extended Data Fig. 2b). An alternative possibility that is consistent with the data could be the effect of the different inducers used with the different plasmid backbones: m-toluic acid for RSF1010 derived plasmid and arabinose for the oriR101 derived plasmid. We find that increasing concentrations of m-toluic acid have a negative effect on bacterial growth (Extended Data Fig. 2c). We do not exclude an additional effect of the plasmid copy number. Next, we optimized arabinose concentration (Extended Data Fig. 2d). Finally, we also studied the stability of the genetic system with retrons arrays of different length using a 5-day protocol in the presence or absence of the inducer (Extended Data Fig. 2e,f). Sequencing of the whole retron array harboring 2, 3 or 5 msds with different donors revealed that in most cases more than 80% of the colonies preserve an intact retron array after 5 days showing the robustness of the multitron technology.

With curable, single-plasmid parameters optimized, we next attempted to isolate clones that were simultaneously edited at distant regions of an individual genome (*fbaH* and *hda*). We found substantial editing of each target (~20%) and additionally found that the efficiency of editing could be increased to ~45% with an additional day of editing, demonstrating the continuous nature of this approach (Fig 4c). Following editing, we cured the temperature sensitive editing plasmid from 96 individual colonies (48 after 24 hours and 48 after 48 hours) and sequenced the editing loci from each colony. The overall rates of editing at both sites and time points from the individual colonies closely matched the bulk sequencing data (Fig 4c). We also calculated the expected frequency of finding doubly edited colonies based on the product of the bulk rates at each site and found that the real frequency of doubly edited colonies (~4% after 24 hours and ~22% after 48 hours) was exactly reflected in the real colony sequencing (Fig 4d).

We also investigated the background mutation rate of multitrons to evaluate the usefulness of the method when fidelity is required. Specifically, we measured the accumulation of local and global off-target mutations in E. coli bMS.346 genome in the presence or absence of RT activity. First, we constructed a dead RT version of the multitron targeting fbaH and hda genes which showed eliminated effective precise editing (Extended Data Fig. 3a). Local off-target mutations were quantified by analyzing the 70 bp homology window of fbaH and hda donors in the chromosome for unintentional mutations. We found no difference in mutation frequency in the donor window in the live versus dead RT condition (approximately 5×10⁻⁵ errors/base, consistent with Illumina sequencing error; Extended Data Fig. 3b). Global off-target mutations were measured by comparing whole-genome sequencing of colonies after recombineering against with the parental strain. We found three mutations across the colonies in the live RT version (one of which appears to be a longer homologous recombination event between the plasmid araC and the genome araC) versus two mutations across the colonies in the dead RT version (Supplementary Table 2). The number of mutations is below what has been found previously with CspRecT alone (4 off-target mutations per genome)³³, so we conclude that the retron component is not adding substantively to off-target mutations.

Metabolic Engineering in Bacterial Genomes Using Multitrons

We next pushed toward a proof-of-concept use of multitrons in metabolic engineering by modifying bacterial genomes. First, we next assessed the ability of re-optimized, temperature-sensitive arrayed msd multitrons to simultaneously edit five positions (*hda*, *fbaH*, *priB*, *rpoB* and *gyrA*). All sites were precisely edited after 24h, and editing continued to increase over the next 24h following a passage, illustrating the continuous nature of the retron-derived editing (Fig 5a).

To test multitrons in the context of metabolic engineering, we chose to focus on increasing production of lycopene by modifying genes in its biosynthetic pathway (Fig 5b). We selected eight bacterial genes which have been shown to affect lycopene yield^{3,37–39} (Fig 5b). Five of them (*dxs, idi, ispA, ispC, rpoS*) were subjected to modification of their RBS regions to enhance their similarity to the canonical Shine-Dalgarno sequence

(TAAGGAGGT)⁴⁰. The other three genes (*gmpA*, *gdhA*, *fdhF*) were specifically targeted for inactivation by the introduction of premature stop codons within their open reading frames.

We established a general workflow for metabolic engineering using multitrons (Fig 5c; Material and Methods). The multitron plasmid (MP) was generated using a one-pot golden gate approach⁴¹ to clone arrayed msds encoding different donors. The MP was next transformed into the bacterial host harboring the lycopene plasmid (LP, a plasmid containing three essential genes (*crtE*, *crtI*, *crTB*) required for lycopene production⁴². Editing cycles were carried out at the permissive temperature (30°C), with dilutions of the culture after every cycle. Editing targets were sequenced in bulk using Illumina MiSeq to determine overall efficiencies. In parallel, cells were plated at 37°C to cure the MP. Finally, red colonies (indicative of lycopene) from the plates were selected for further quantification of lycopene production levels (Fig 5c).

In total, we tested six different arrayed msd multitrons across this workflow, containing target gene donors in combinations that have been have been shown to increase lycopene yield³. Editing rates were measured after cycles 1 and 3 of editing (24h and 72h, respectively) showing values that increase with time (Fig. 5d). After 72h of editing, the precise editing rates when making one or two mutations ranged from 10 to 40%. When making three or five mutations, editing rates were lower, which could be due to the known negative fitness effect³ of these mutations on the bacterial growth (Fig 5d).

We measured relative lycopene production from 84 isolated red colonies after plating cultures on LB agar plates after editing (Fig 5e). In each case other than the control, individual colonies produced variable amounts of lycopene, likely resulting from the intended genotypic diversity generated by the editing. As an example, the most productive isolate after RBS optimization of dxs and idi genes increased lycopene production by more than 400% of control values, there was a second production cluster around 300% of control, and a final cluster around 200% of control (Fig 5e). We reasoned that these three different clusters may represent a single dxs mutation, a single idi mutation, and both together. To test that hypothesis, a representative of each cluster was selected and re-streaked for colonies, which were re-measured for lycopene and Sanger sequenced. Indeed, that the best producing isolate carried RBS mutations of both dxs and idi genes, second-best had only the dxs mutation, and the third-best had only the idi mutation (Fig 5f). This proof-of-concept was achieved with a single cloning reaction (one-pot Golden Gate) to generate a single plasmid and one course of editing, creating both single mutants and the double mutant. To generate this same result without multiplexing would require cloning two distinct editors for each of the sites, running parallel editing, genotyping, and quantification on each single edit. Then, curing the plasmid from an edited clone, adding the opposite plasmid to make the other edit, running another editing course, and finally quantifying the double mutant. Thus, a multiplexed experiment generates a diversity of genotypes and corresponding phenotypes across multiple sites simultaneously.

Multitrons with CRISPR Editing in Eukaryotic Cells

Given the success of the arrayed msd multitron in recombineering, we next sought to expand the utility of this technology to eukaryotic cells. Retron RT-Donors have been used in

S. cerevisiae in combination with CRISPR Cas9 and gRNAs to install precise mutations via templated repair of a cut site (Fig 6a; Extended Data Fig. 4a). The architecture of the donor element in yeast is typically a retron ncRNA fused to a CRISPR gRNA and scaffold, all surrounded by ribozymes to excise the editing elements from an mRNA. Given the goal of engineering a eukaryotic msd array, the relatively large, structured ribozymes present a potential engineering hurdle if they need to be multiply duplicated. Therefore, we first tested replacement of the ribozymes with Csy4 recognition sites and Csy4 nuclease expression by comparing a singleplex retron-derived precise editor of the ADE2 locus in the standard arrangement using ribozymes against an alternate version in which the flanking ribozymes were replaced by Csy4 recognition sites. In both cases, we tested editing with or without the inclusion of a Csy4 gene in an integrated, inducible, genomic cassette that also expresses the retron RT and Cas9. We found, as expected, no effect of Csy4 expression on the ribozyme version of the precise editor, but a dramatic effect of Csy4 expression on the alternate version with Csy4 sites. Precise editing nearly matched the efficiently of the ribozyme version with Csy4 expression, but was sharply reduced in its absence, indicating that processing of the non-coding elements is required and can be achieved using Csy4 (Fig 6a).

We next tested a eukaryotic multitron based on an array of ncRNA/gRNAs targeting *ADE2* and *FAA1* for precise mutations of three base pairs each. For each site, the ncRNA encoding the donor for the site was fused to the gRNA for the same site. The two sites were separated by a Csy4 recognition site and the double ncRNA/gRNA array was surrounded by ribozymes (Fig 6b). Both sites were edited to nearly 100% in the presence of Csy4 expression, and we observed low indel rates that were similar between the ribozyme- and Csy4-processed cassette (Extended Data Fig. 4a,b). In the absence of Csy4, in contrast, the *FAA1* site was edited to nearly 100%, while the *ADE2* editing was sharply reduced. In our multitron, the *ADE2* donor/gRNA was in the first position, suggesting that Csy4 processing is required on the 3' end, adjacent to the gRNA scaffold, but dispensable on the 5' end, adjacent to the msr.

Analogously to our bacterial editors, we verified that edits accumulate on genomes according to the product of the rates at each site. To this end, we compared bulk editing rates across the *ADE2* and *FAA1* sites to rates of edits in individual colonies. As in the bacterial experiments, colony sequencing matched bulk sequencing for both individual sites and for the expected frequency of double edits. We found that virtually all of the colonies sequenced contained the precise edits intended, consistent with the rates inferred from bulk Illumina amplicon sequencing (Fig 6c,d).

It is preferable to minimize the donor/gRNA unit for practical reasons of construction, just as in the prokaryotic version. Therefore, in a parallel to the prokaryotic msd array multitron, we engineered a eukaryotic msd/gRNA array multitron, transferring the msr to a distinct transcript to reduce editing unit size and avoid long direct repeats (Extended Data Fig. 4c). This enabled construction of multitrons of arbitrary size using efficient one-step golden gate cloning. The msd encoding the donor remains fused to its matched gRNA, while a trans msr is able to function as a primer to create the RT-Donor internally (Extended Data Fig. 4d). We tested versions of this eukaryotic arrayed msd/gRNA multitron to precisely edit two, three,

or five non-adjacent sites simultaneously (Fig 6e,f; Extended Data Fig. 4e). In each case, all targeted sites were edited, with precise edits and indels increasing over time (Extended Data Fig. 4f–h).

Finally, we sought to test whether the engineered eukaryotic msd/gRNA array multitron would enable precise genome editing in human cells. We adapted an approach for multiplexing pegRNA expression¹⁴, described initially to enable multiplexed prime and base editing, to enable the expression and processing of multiple retron msds and a single retron msr in trans. This yielded expression cassettes analogous to those developed for yeast editing, with tRNAs driving the processing of the msd/gRNA cassettes. We found that these engineered cassettes enabled the simultaneous precise edits of three non-adjacent sites in the human genome, from a single plasmid, in cultured HEK293T human cells (Fig 6g). Taken together, our data shows that the arrayed msd multitron with trans msr is a generalizable strategy for multiplexing edits within a genome.

DISCUSSION

This work demonstrates the construction, optimization, and use of multitrons for multiplexed precise editing within genomes of prokaryotic and eukaryotic cells. Final versions make use of donor-encoding retron msd arrays. Critically, we engineered the msd array format by optimizing not only for editing efficiency, but also for enabling practical cellular and molecular workflows. The compact multitron form is compatible with single-plasmid designs, one-step golden gate assembly, and plasmid removal in prokaryotic cells. These features should permit widespread adoption of the multitron editing approach. A concurrent work has shown a similar approach, providing independent validation of the utility of multiplexed retrons for recombineering ⁴³.

We demonstrate simultaneous editing of up to five sites, with replacements of up to 8 base pairs per site, and deletions of up to 100 bases. This approach builds on previous work using oligonucleotides for MAGE by enabling efficient multisite editing without repeated transformations and by enabling a user to specify distinct combinations of donors per cell rather than relying on the random segregation of electroporated oligos. Multitrons enable a wider range of precise mutations than multiplexed base editors, and a more compact and simplified form than multiplexed prime editors.

We found that the rate of combinatorial editing on a single genome was predicted by product of rates at each individual site. As the number of editing sites increased, the rate at each site decreased. Thus, for 4+ edits, the rate of achieving all mutations on a single genome can drop well below 1:1,000. Whether his rate is high enough will depend on the application. For instance, if edited cells are to be subjected to a selective phenotyping assay, the fact that combinatorial mutants are present in the population, even at low rates, is sufficient to enable quantification of enrichment or depletion. If however, one needs to isolate a clone without phenotypic selection, we would recommend limiting the edits per round of editing to ≤ 3 at this time. Further development of the technology or the addition of simultaneous counter-selection will help drive the practical number of edits up in the future.

For contextualization to other technologies, one alternative is base editing, which can also be multiplexed. On the upside, Base Editors can reach efficiencies of over 80%¹³ and can be multiplexed to more than 30 loci¹⁴. However, it is important to note that only 2 of the 14 edits we made in bacteria and none of the edits made to yeast are suited to base editing. The deletions and RBS modifications that we made are a particularly salient example of a place where base editors fall short. MAGE is a more relevant comparison to the bacterial work and can achieve similar efficiencies, although with dramatically more hands on type to complete the multiple electroporation cycles. However, MAGE cannot be used to make the edits that we show in yeast or human cells (new to the revision) so as a technology, we would argue that the multitrons are a more universal platform.

The existing yeast genome editing toolbox is vast and spans from simple HR-based editing to more nuanced, multiplexed approaches that have enabled both trackable, genome-wide phenotypic screens and targeted, saturation mutagenesis of individual ORFs^{44–50}. However, "trackable and multiplex" in this context has usually meant many changes across many genomes, with ≤1 change per genome, rather than >1 changes on an individual genome; and tools that do enable multiple changes per single genome typically do not support trackability of precise and varied edits, or require involved and time-consuming workflows. In this sense, we believe that multitrons, in their ability to support multiple trackable and precise edits per individual genome, will naturally fit into the toolbox of yeast biologists in years to come.

We demonstrate proof-of-concept uses in molecular recording, genetic element minimization, and metabolic engineering. Future development will likely push the scale of multitrons both in the number of simultaneous mutations and the diversity of combinatorial mutations using libraries targeting two or more sites.

METHODS

Biological replicates were taken from distinct samples, not the same sample measured repeatedly.

Plasmid Construction

All the plasmids used in this work are listed in Supplementary Table 3. Furthermore, all the RT-donors and the oligonucleotides containing the desired mutations for the editing experiments are listed in Supplementary Table 4.

E. coli—To clone additional 70 bp donors in a single msd, pSLS.492²⁹ plasmid containing a *rpoB* donor was used as backbone. To clone a donor upstream of the *rpoB* donor, a 60 bp reverse oligo annealing (25bp) with the 5' region of the msd and containing 35 bp of the new donor, and a 60 bp forward oligo annealing (25bp) with the 5' end of *rpoB* donor and harboring the other half of the new donor were used. To clone a donor downstream of the *rpoB* donor, a 60 bp forward oligo annealing (25b) with the 3' region of the msd and containing 35 bp of the new donor, and a 60 bp reverse oligo annealing (25bp) with the 3' end of *rpoB* donor and harboring the other half of the new donor were used. After a 30 cycles PCR reaction with Q5 hot-start high-fidelity polymerase (NEB) following

recommended vendor protocol, a KLD reaction (NEB) was carried out to self-ligate the plasmid encoding an additional donor.

To construct the plasmids harboring the retron arrays in their different architectures the pCDF-DUET-1 vector (Novagen) was used as a backbone. A parental plasmid (pAGD159; Supplementary Table 3) containing a whole ncRNA with a *gyrA* donor downstream of the first T7 promoter, and Eco1-RT downstream of the second T7 promoter was constructed. To assess whole ncRNA retron arrays, the ncRNA harboring the *rpoB* donor from pSLS.492 was amplified and cloned upstream and downstream of the *gyrA*-containing ncRNA by Gibson Assembly. To construct the plasmids containing the msd array, firstly, the msr was deleted from pAGD159 and subsequently cloned between the second T7 promoter and Eco1-RT using a Gibson Assembly approach. Finally, the msd harboring the *rpoB* donor from pSLS.492 was amplified and cloned upstream and downstream of the *gyrA*-containing ncRNA by Gibson Assembly. To test if the msd array could act as a single transcript unit independent of the msr region, a T7 terminator was cloned between the msd array and the second T7 promoter.

To construct multitrons containing more than 2 arrayed msd a one-pot Golden Gate cloning approach was used. Firstly, a plasmid containing a sfGFP stuffer flanked by two inverted BsaI (type IIS restriction enzyme) target sites were cloned in the place of the msd Array generating pAGD236 (see Figure 4c for reference). Editing units, based on a msd with a donor were order as gBlocks (IDT) flanked by inverted BsaI target sites and compatible nucleotide overhangs to clone them in tandem. The Golden Gate protocol was carried out in 20uL reactions as follows: 1 uL pAGD236, 5uL of each gBlock (3uL for 5x msd arrays), 1.5uL BsaI (NEB), 2uL T4 DNA ligase Buffer, 0.5 uL T4 DNA ligase (NEB). The reaction consists on 30 or 60 cycles (depending on the complexity) of 5 min at 16°C and 5 min at 37°C and a final cycle of 10 min at 60°C.

To optimize multitrons for metabolic engineering, the retron cassette (ncRNA and RT) from pSLS.492 was cloned into pORTMAGE-Ec1³³ upstream of the CspRecT gene (Extended Data Fig. 2a). RBS optimization of Eco1 RT and CspRecT genes were carried out using primers that contain the optimized RBS and self-ligating the plasmids using KLD reaction mix. Finally, recombineering operon was cloned into pKD-46³⁵ backbone to obtain the parental temperature-sensitive multitron plasmid (pAGD248). Multitron msd array architecture with the sfGFP stuffer flanked by two inverted BsaI described previously was cloned into pAGD248 generating pAGD335. The golden gate reaction was used to clone gBlocks containing the donors into the pAGD335 backbone to generate the multitrons versions used in Fig 4.

S. cerevisiae—To assess whether Csy4 could enable the processing of editrons and retron msd/Cas9 gRNA units for genome editing, pSCL390, a derivative of pZS.157 (Addgene #114454), was generated with a yeast codon-optimized P2A-Csy4 CDS gblock (IDT) cloned downstream of the SpCas9 CDS by Gibson Assembly.

To compare the genome editing efficiencies of ribozyme-processed editrons to Csy4-processed editrons, pSCL.396, a derivative of pSCL.39 (Addgene #184973), was generated

with the 5' Hammerhead ribozyme and 3' HDV ribozyme replaced by Csy4 recognition sites by amplification of the editron and backbone from pSCL.39 and assembled via Gibson Assembly.

To assess whether Csy4 could enable the processing of arrayed editrons, we generated pSCL.391, a derivative of pSCL.39 where a second editron, targeting the *S. cerevisiae FAA1* locus was added on the 3' end of the *ADE2*-targeting editron by Gibson Assembly. The cassette thus consists of two editrons, separated by a Csy4 recognition site, and flanked by a Hammerhead ribozyme and a HDV ribozyme on the 5' and 3' of the expression cassette, respectively.

To construct plasmids for the expression of retron msd arrays, first, a Golden Gate compatible entry vector, pSCL.452 was generated that carries the Gal7 promoter and terminator, alongside a cassette for expression of the retron msr from a Pol III SNR52 promoter. pSCL.452 is a derivative of a derivative of pSCL.39, generated by Gibson Assembly of the pSCL.39 backbone, amplified to replace the recombitron with inverted PaqCI sites for Golden Gate assembly, with a gblock (IDT) encoding pSNR52p-msr-SUP4t.

Next, plasmids carrying retron msd arrays for the editing of multiple loci in the yeast genome were generated by Golden Gate cloning of pre PaqCI-digested pSCL.452 with gBlocks (IDT) that encoded a PaqCI cut site, a retron msd-encoded donor and paired gRNA for editing, a Csy4 recognition sequence, and a PaqCI cut site (Fig 6e). gBlocks were ordered with compatible nucleotide overhangs to enable random cloning of all combinations of gblocks into the entry plasmid, after PaqCI digestion. We ordered gblocks to edit the *ADE2*, *FAA1*, *TRP2*, *SGS1* and CAN1 loci. These were cloned into the PaqCI-digested pSCL.452 backbone by Golden Gate cloning, yielding plasmids pSCL.473 (editors for *ADE2*, *FAA1*), pSCL.475 (editors for *ADE2*, *FAA1*, *TRP2*, *SGS1* and *CAN1*).

H. sapiens—All human vectors are derivatives of pSCL.273, itself a derivative of pCAGGS⁵¹. pCAGGS was modified by replacing the MCS and rb_glob_polyA sequence with an IDT gblock containing inverted BbsI restriction sites and a SpCas9 tracrRNA, using Gibson Assembly. The resulting plasmid, pSCL.273, contains an SV40 ori for plasmid maintenance in HEK293T cells. The strong CAG promoter is followed by the BbsI sites and SpCas9 tracrRNA.

BbsI-mediated digestion of pSCL.273 yields a backbone for single or library cloning of plasmids with inserts that contain {retron RT – H1 promoter – hCtRNA_n_msdRNA_n_gRNA_n}, by Gibson Assembly or Golden Gate cloning (see Fig 6e for an illustration of this principle). The retron RT (or its catalytically dead counterpart) and H1 promoter fragments were synthesized through IDT, as were the hCtRNA_n_msdRNA_n_gRNA_n units. Golden gate cloning of these elements alongside 3 editor units (*EMX1*, *FANCF*, and *HEK3*) yielded plasmids pSCL.757 (CAGp-Eco3RT-TYpA // H1-msr-tRNA-Cys-GCA-*EMX1*_msd-gRNA); pSCL.758 (CAGp-Eco3RT-TYpA // H1-msr-tRNA-Cys-GCA-*HEK3* msd-gRNA-

tRNA-Cys-GCA-*FANCF*_msd-gRNA-tRNA-Cys-GCA-*EMX1*_msd-gRNA) and pSCL.760 (CAGp-dEco3RT-TYpA // H1-msr-tRNA-Cys-GCA-*EMX1* msd-gRNA).

Strains and Growth Conditions

All bacterial and yeast strains are listed in Supplementary Table 5.

Bacterial Strains—The *E. coli* strains used in this study were DH5α (New England Biolabs) for cloning purposes, bMS.346 (DE3) for retron recombineering assays. Bacteria were grown in LB medium (10 g/l tryptone, 5 g/l yeast extract, 5 g/l NaCl). Antibiotics were added as required (carbenicillin, spectinomycin, kanamycin and chloramphenicol).

Yeast Strains—All yeast strains were created by LiAc/SS carrier DNA/PEG transformation⁵² of BY4742²⁶. Strains for evaluating the effect of Csy4 on genome editing efficiency were created by BY4742 integration of plasmids pZS.157 (Addgene #114454) or pSCL.390. The plasmids were KpnI-linearized and inserted into the genome by homologous recombination into the *HIS3* locus. Transformants were isolated on SC-HIS plates.

Bacterial Recombineering expression and analysis

In multitron experiments edit bacterial genomes, the retron cassette encoded in a pET-21 (+) plasmid (Novagen) and the CspRecT and mutLE32K in the plasmid pORTMAGE-Ec1³³ were overexpressed using 1 mM IPTG, 1 mM m-toluic acid and 0.2% arabinose for 16 h with shaking at 37°C. For the molecular recording assay (Fig 1g), a control without m-Tol and different concentration of the inducer, ranging from 0,005 mM to 0,1 mM, were added. To engineer the lycopene metabolic pathway (Fig 4), bMS.346 electrocompetent cells containing pAC-LYC⁴² plasmid, were transformed with different multitron plasmid versions (Supplementary Table 3 and 4). and growth for 16 h at 30°C. Single colonies from the transformation plate were inoculated into 500uL of LB in triplicates in 1mL deep-well plates and incubated at 30°C for 24 h with vigorous shaking to prevent the cells from settling. A 1:1000 dilution of the cultures were passaged into LB 1% arabinose and incubated at 30°C for 24 h with vigorous shaking. This step was repeated for a total of 72h.

After the different type of assays carried out in this study, a volume of 25 ul of culture was collected, mixed with 25 ul of water and incubated at 95°C for 10 min. A volume of 1 ul of this boiled culture was used as a template in 30-ul reactions with primers flanking the edit site, which additionally contained adapters for Illumina sequencing preparation (Supplementary Table 6). These amplicons were indexed and sequenced on an Illumina MiSeq instrument and processed with custom Python software to quantify the percentage of precisely edited genomes.

Yeast editing expression and analysis

The parental strains (-Csy4: HIS3::pZS.157; +Csy4: *HIS3*::pSCL390) were transformed with variants of the editron expression cassettes by LiAc/SS carrier DNA/PEG transformation. Single colonies from the transformation plate were inoculated into 500uL of SC-*HIS-URA* 2% raffinose in triplicates in 1mL deep-well plates and incubated at 30°C for 24 h with vigorous shaking to prevent the cells from settling. Cultures were passaged

into SC-HIS-URA 2% galactose and incubated at 30°C for 24 h with vigorous shaking. This was repeated once more for experiments meant to compare the genome editing efficiencies of ribozyme-processed editrons to Csy4-processed editrons, for a total of 48h of editing; and four more times for experiments meant to assess whether arrays of retron msds could be used to edit multiple loci in the yeast genome, for a total of 120h of editing. At each timepoint of galactose-induced editing, a 250uL aliquot of the cultures was harvested, pelleted and washed with water, and prepped for deep sequencing of the loci of interest.

To compare the bulk editing rates across sites to rates of edits in individual colonies for the Csy4-processed editrons, after 48h of editing, dilutions were plated on SC-HIS-URA plates. For each of 3 biological replicates, 10 colonies were grown overnight in SC-HIS-URA to saturation and subjected to genomic DNA extraction and targeted PCR of the ADE2 and FAA1 loci, as described below. Amplicons were sent for Sanger sequencing, and editing rates per biological replicated were calculated by assessing the Sanger reads for the 10 colonies per biological replicate for the expected precise edit.

Samples were prepped for deep sequencing of the edited loci as described previously²⁹. Briefly, genomic DNA was extracted by (1) resuspending the cell pellets in 120uL of lysis buffer (100 mM EDTA pH 8, 50 mM Tris-HCl pH 8, 2% SDS) and heating them to 95 °C for 15 min; (2) cooling the lysate on ice and adding 60uL of protein precipitation buffer (7.5 M ammonium acetate), then inverting gently and placing samples at -20°C for 10min; (3) centrifugation of the samples at maximum speed for 2mins (or until a clear supernatant forms) and collecting the supernatant (~100uL) in new 1.5mL tubes; (4) precipitating the nucleic acids by adding equal parts of ice-cold isopropanol to the samples, mixing the samples thoroughly and incubating the mix at -20°C for 10min (or overnight for higher yield), followed by pelleting by centrifugation at maximum speed for 2min; (5) washing the pellet twice with 200 µl of ice-cold 70% ethanol, followed by air-drying it; and (6) resuspending the pellet in 40 µl of water. 0.5 uL of gDNA was used as template in 20-µl PCR reactions with primers flanking the edit site in of the target locus, which additionally contained adapters for Illumina sequencing preparation (Supplementary Table 6). Importantly, the primers do not bind to the retron msd donor sequence. These amplicons were indexed and sequenced on an Illumina MiSeq instrument and processed with custom Python software to quantify the percentage of precise edits using the retron derived RT-DNA template.

Human Cell Culture

HEK293T cells, expressing spCas9 from a piggyBac integrated, TRE3G driven, doxycycline-inducible (1 μ g/ml) cassette¹⁸, were seeded at 7 \times 10⁵ live cells/well in coated 6-well plates and grown in DMEM +GlutaMax supplement (Thermo Fisher #10566016) overnight. Lipofectamine 3000 transfection mixes were prepared in independent triplicates and cells were transfected with 5ug of plasmid per well (3 wells per plasmid). Cells were passaged the next day and doxycycline was refreshed at passaging. Cells were grown for an additional 48 h, for a total of 72h of editing. Three days after transfection, cells were collected for sequencing analysis. To prepare samples for sequencing, cell pellets were collected, and gDNA was extracted using a QIAamp DNA mini kit according to the

manufacturer's instructions. DNA was eluted in 150 µl of ultra-pure, nuclease-free water. 0.5 µl of gDNA was used as template in 20-µl PCR reactions with primers flanking the edit site in of the target locus, which additionally contained adapters for Illumina sequencing preparation (Supplementary Table 6). Importantly, the primers do not bind to the retron msd donor sequence. These amplicons were indexed and sequenced on an Illumina MiSeq instrument and processed with custom Python software to quantify the percentage of precise edits using the retron derived RT-DNA template.

Whole-Genome Sequencing to Measure Off-Target Mutagenesis.

A total of 7 genomes were sequenced using a shot-gun approach: *E. coli* bMS.346 parental strain, 3 individual colonies after one recombineering round using a wild-type Eco1 RT and 3 individual colonies after one recombineering round using a dead Eco 1 RT. Prior to sequencing, 3 ml LB liquid culture of each isolate was grown for 16h at 37°C. The gDNA was isolated by using the Quick-DNA/RNATM Miniprep Plus Kit (Zymo Research). Extracted gDNA was measured using QubitTM 1X dsDNA High Sensitive (HS; Thermo Scientific). gDNA was tagmented using Tn5 transposase using the following reaction (50uL): 25 uL 2x TD Buffer (20 mM Tris-HCl pH 7.6, 10 mM MgCl2 and 20% dimethyl formamide), 2.5uL Tn5 (in-house prepared) and 50 ng gDNA. The reaction was incubated for 1h 30° at 37 °C. The gDNA was cleaned-up and eluted in 15uL using the DNA Clean & Concentrator (Zymo Research). Tagmented gDNAs were indexed and sequenced on an Illumina MiSeq instrument. *E. coli* strain bMS.346 whole genome variants were called against *E. coli* K12 sbstr. MG1655 genome (accession no. NC_000913) using Geneious Prime® 2023.2.1 software alignment tools. Variants appearing in the genome of the wild-type and dead RT isolates were called against the bMS.346 parental strain.

Colorimetric screen and assay for lycopene production.

After cycle 3 (72h) of the metabolic engineering assay, cells from the edited bMS.346 populations using different multitrons were plated on LB-chloramphenicol agar plates and grown for 1 day at 30°C and 2 days more in darkness and at room temperature to produce red colonies. Per edited population with a multitron, plates containing around 10^3 colonies were screened by visual inspection searching for increased red colour intensity. A total of 84 colonies (12 isolates from each multitron version and 12 from the control) were selected for lycopene quantification. These isolated colonies were grown into 1 mL LB-chloramphenicol in 1 mL deep-well plates for 24 h at 37°C to cure multitron plasmid. For lycopene extraction, 1 ml of cells were centrifuged at 16,000g for 30 s, the supernatant was removed and the cell pellet was resuspended with 1 mL water. Cells were re-centrifuged at 16,000g for 30 s, the supernatant was removed and the cells were resuspended in 200 ml acetone and incubated in the dark for 15 min at 55 °C with intermittent vortexing. The mixture was centrifuged at 16,000g for 1 min and the supernatant containing the lycopene was transferred to 96 white/clear bottom plate. Absorbance at 470 nm of the extracted lycopene solution was measured using a spectrophotometer to determine the lycopene content. Lycopene yield of the different colonies from each was calculated by normalizing the times of lycopene production against the control. Cells coming from different clusters of lycopene production were re-striked in LB-chloramphenicol agar plates grown for 24h at 30°C and for another 48h at room temperature. Between 3 and 8 colonies from each re-

striking were selected to quantify the lycopene production following the described protocol and for Sanger sequencing across the *dxs/idi* targets.

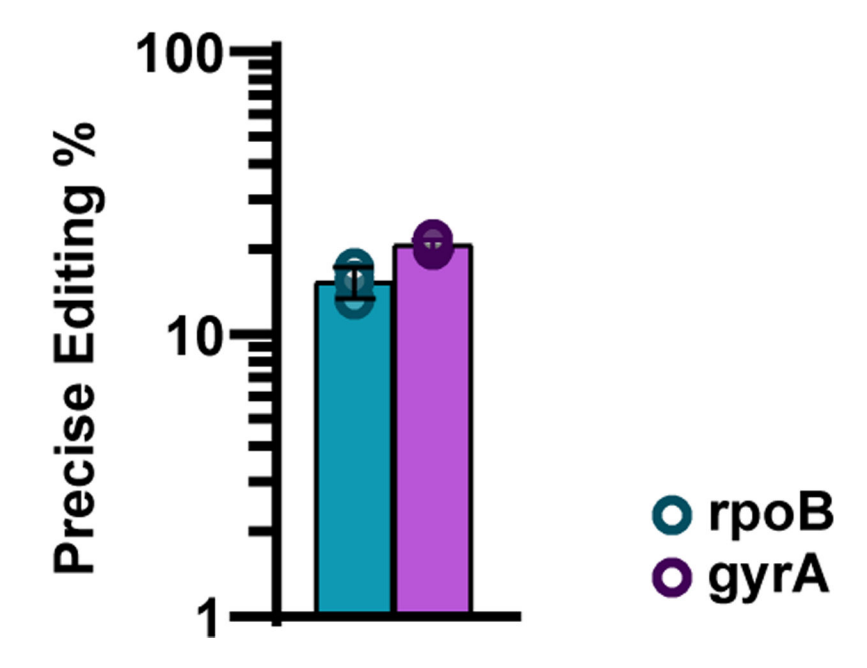
Assessment of plasmid stability

E. coli—Recombineering plasmid was transformed into *E. coli* strain bMS.346, followed by 5 days of growing and diluting in the presence or absence of the arabinose. A dilution of the final culture was diluted and plated. Finally, the msd Array of 10 individual colonies per replicate (n=3) were amplified and sequenced to assess genetic stability of the multitron approach (see Extended Data Fig. 2f for reference).

S. cerevisiae—Three individual colonies of yeast carrying 2, 3 or 5 donor arrayed retron msdRNA-Cas9 gRNA expression cassettes were inoculated in SC-*URA-HIS* 2% Raffinose media, and passaged 5 times overnight in SC-*URA-HIS* with 2% Galactose, for a total of 120h of editing at 30C. After 120h of editing, dilutions were plated on SC-*HIS-URA* plates and 10 colonies for each biological replicates were subjected to plasmid extraction. Plasmids were sent for whole-plasmid sequencing and consensus reads were aligned to the reference plasmid.

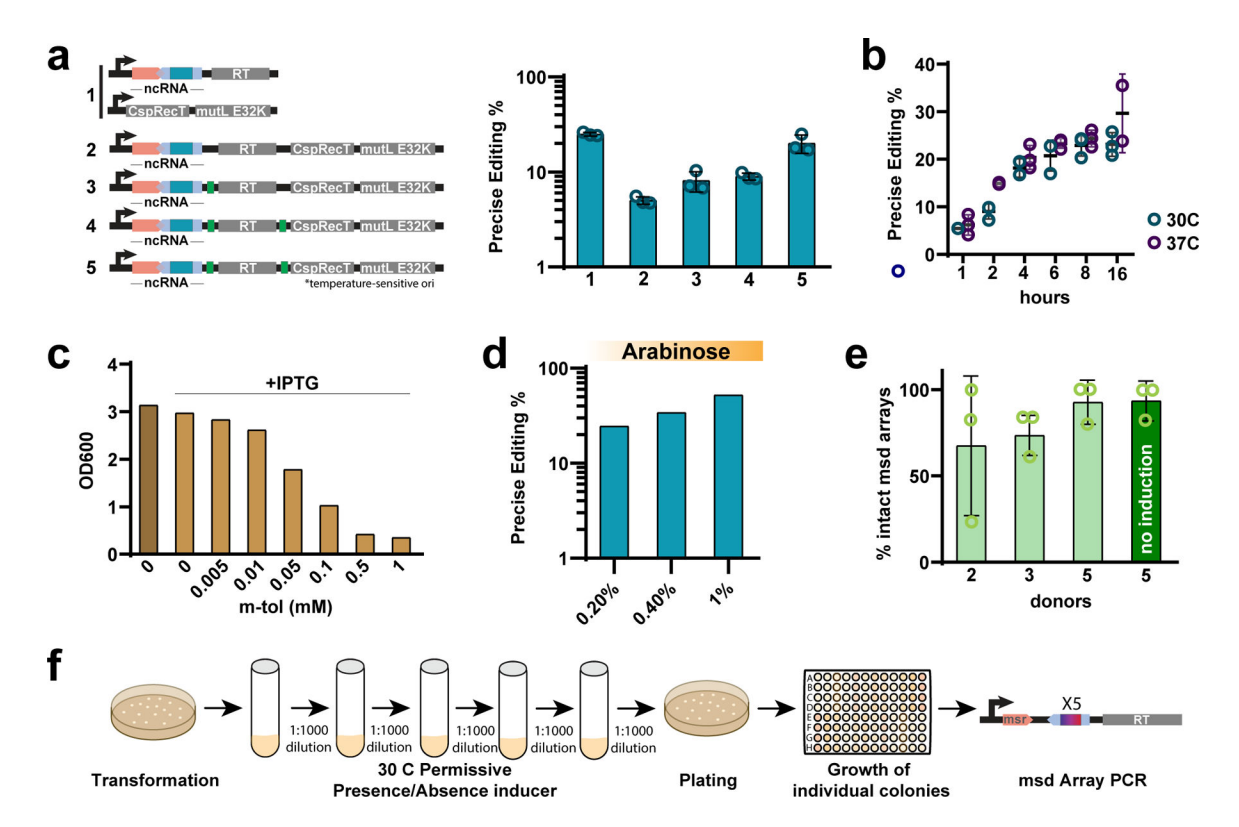
Extended Data





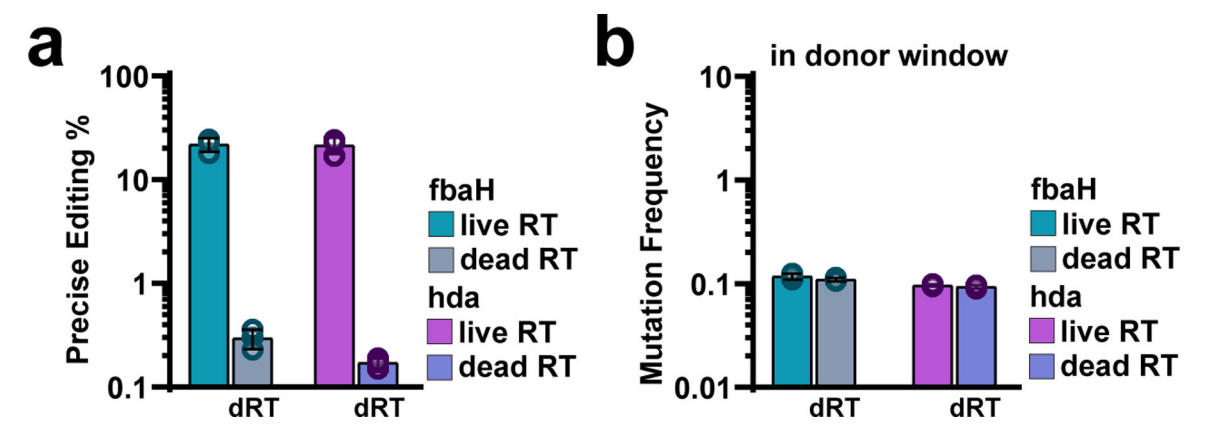
Extended Data Fig. 1 |. Trans *msr* multitron architecture enables precise genome editing. Top: Schematic of retron recombineering using an *msd* array with a single msr sequence in trans including a terminator (T) between the *msd* array and *msr*. Bottom: quantification

of precise editing rates for precise editing of rpoB or gyrA simultaneously by Illumina sequencing after 24 h of editing. Circles show each of the three biological replicates, bars are mean \pm SD.



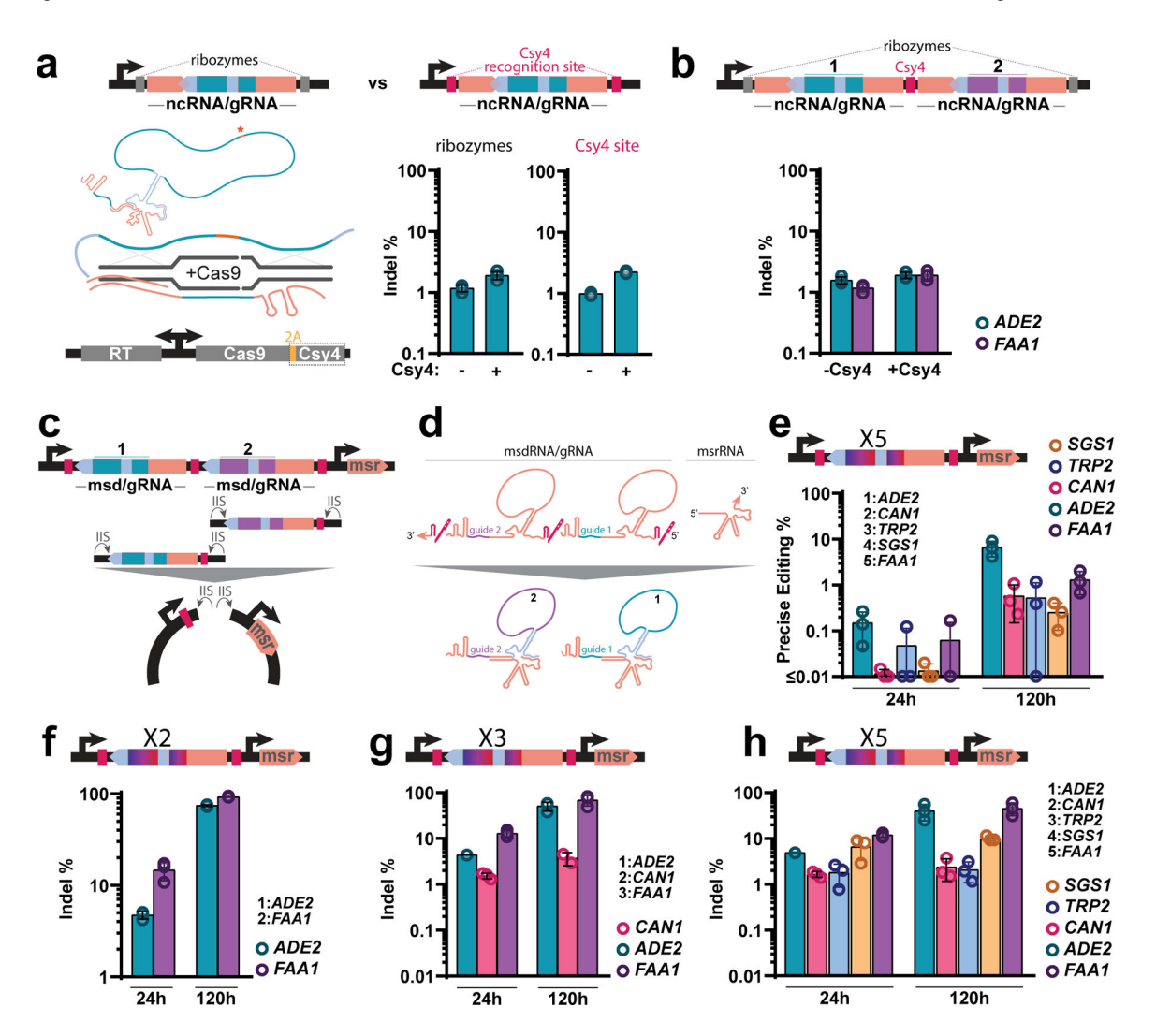
Extended Data Fig. 2 |. Optimization of retron recombineering using a single plasmid.

a. Left: schematic of the different retron operon architectures tested. ncRNA with donor (orange and blue), genes required (grey) and optimized ribosome binding sites (RBS) regions (green) are indicated Right: quantification of rates for precise rpoB editing, circles show each of the three biological replicates, bars are mean \pm SD. **b.** Quantification of precise editing rates for rpoB target site at 30 and 37°C, circles show each of the three biological replicates, lines are mean \pm SD. c. Quantification of OD600 using increasing concentrations of m-toluic acid after 16 h of bacterial growing (n = 1). **d.** Quantification of precise editing rates for rpoB using different concentrations of arabinose (n = 1). e. Quantification of colonies with intact msd arrays. A total of 30 colonies coming from 3 different replicates were sequenced, bars are mean \pm SD All precise editing rates were quantified using Illumina MiSeq after 24 h of editing. f. Scheme of the protocol used to analyze genetic stability of the retron arrays. Briefly, recombineering plasmid was transformed into E. coli strain bMS.346, followed by 5 days of growing and diluting in the presence or absence of the arabinose. A dilution of the final culture was diluted and plated. Finally, the msd Array of 10 individual colonies per replicate (n = 3) were amplified and sequenced to assess genetic stability of the multitron approach.



Extended Data Fig. 3 |. Local off-target mutations.

a. Quantification of precise editing rates for fbaH and hda genes using a live or dead version of Eco1 RT, circles show each of the three biological replicates, bars are mean \pm SD. b. Local off-target mutation frequency in the 70 bp region of the chromosome homologous to fbaH and hda editing donors using a live of dead version of Eco1 RT circles show each of the three biological replicates, bars are mean \pm SD. All data was quantified using Illumina MiSeq after 24 h of editing.



Extended Data Fig. 4 |. Intended and undesired on-target mutation ratesceaused by arrayed retron multiplexed editing in yeast cells.

a. Top: Schematic of the donor encoding retron ncRNA/gRNA expression cassette expressed from a Gal7 Pol II promoter and flanked by ribozymes versus a new construction replacing ribozymes with Csy4 sequences. Bottom left: schematic of a retron ncRNA-Cas9 gRNA hybrid for genome editing in yeast, depicted above the protein-coding expression cassette which is inserted into the yeast genome. Bottom right: quantification of indel rates of the *ADE2* locus in yeast by Illumina sequencing after 48 h of editing. Circles show each of the three biological replicates, bars are mean ± SD; absence/presence of Csy4 in the protein-coding expression cassette is shown below the graph. **b.** Top: schematic of an arrayed retron ncRNA-Cas9 gRNA expression cassette, expressed from a Gal7 Pol II promoter, flanked by ribozymes, and separated by a Csy4 sequence. The retron editors in positions 1 and 2 target the *ADE2* and FAA1 locus, respectively. Bottom: quantification of indel rates of the *ADE2* and *FAA1* loci in yeast by Illumina sequencing after 48 h of editing. Circles show each of the three biological replicates, bars are mean ± SD; absence/presence of Csy4 in the protein-coding expression cassette is shown below the graph. **c.** Top: schematic of an arrayed retron *msd*RNA-Cas9 gRNA expression cassette, expressed from a Gal7

Pol II promoter, flanked and separated by a Csy4 sequence; the msrRNA is expressed in trans from a SNR52 Pol III promoter. Bottom: assembly schematic for one-pot Golden Gate cloning of multiple *msd*RNA-sgRNA editors. **d.** Schematic showing the presumed processing, annealing and reverse-transcription involved in the generation of editing donors from arrayed retron *msd*RNA-Cas9 gRNA cassettes. **e.** top: schematic of 5x arrayed retron *msd*RNA-Cas9 gRNA expression cassettes, as shown in Extended Data Fig. 4c. Bottom: quantification of precise editing of the various yeast loci targeted by the retron editors shown above, by Illumina sequencing, after 24 and 120 h of editing. The editors target *ADE2*, *CAN1*, *TRP2*, *SGS1* and *FAA1*. Two-way ANOVA, effect of expression time, P = 0.0038. Circles show each 3 biological replicates, bars are mean ± SD. **f–h.** top: schematic of 2x, 3x or 5x arrayed retron *msd*RNA-Cas9 gRNA expression cassettes. Bottom: quantification of indel rates of the various yeast loci targeted by the retron editors shown above, by Illumina sequencing, after 24 and 120 h of editing. Individual open circles show each of three biological replicates per condition, bars are mean ± SD. The editors target *ADE2* and *FAA1* (f); *ADE2*, *CAN1* and *FAA1* (g); and *ADE2*, *CAN1*, *TRP2*, *SGS1* and *FAA1* (h).

Supplementary Material

Refer to Web version on PubMed Central for supplementary material.

Acknowledgements

Work was supported by funding from the National Science Foundation (MCB 2137692), the National Institute of Biomedical Imaging and Bioengineering (R21EB031393), the National Institute of General Medical Sciences (1DP2GM140917), and the UCSF Program for Breakthrough Biomedical Research. S.L.S. is a Chan Zuckerberg Biohub – San Francisco Investigator and acknowledges additional funding support from the L.K. Whittier Foundation and the Pew Biomedical Scholars Program. A.G.-D. was supported by the California Institute of Regenerative Medicine (CIRM) scholar program. S.C.L. was supported by a Berkeley Fellowship for Graduate Study.

Data Availability

All data supporting the findings of this study are available within the article and its supplementary information, or will be made available from the authors upon request. Sequencing data associated with this study is available on NCBI SRA as BioProject ID PRJNA1107632.

References:

- Shalem O, Sanjana NE & Zhang F High-throughput functional genomics using CRISPR-Cas9. Nat Rev Genet 16, 299–311 (2015). [PubMed: 25854182]
- Doench JG Am I ready for CRISPR? A user's guide to genetic screens. Nat Rev Genet 19, 67–80 (2018). [PubMed: 29199283]
- 3. Wang HH et al. Programming cells by multiplex genome engineering and accelerated evolution. Nature 460, 894–898 (2009). [PubMed: 19633652]
- Lajoie MJ et al. Genomically recoded organisms expand biological functions. Science 342, 357–60 (2013). [PubMed: 24136966]
- 5. Nyerges Á et al. Directed evolution of multiple genomic loci allows the prediction of antibiotic resistance. Proc Natl Acad Sci U S A 115, E5726–E5735 (2018). [PubMed: 29871954]

 Barbieri EM, Muir P, Akhuetie-Oni BO, Yellman CM & Isaacs FJ Precise Editing at DNA Replication Forks Enables Multiplex Genome Engineering in Eukaryotes. Cell 171, 1453–1467.e13 (2017). [PubMed: 29153834]

- 7. Isaacs FJ et al. Precise manipulation of chromosomes in vivo enables genome-wide codon replacement. Science 333, 348–53 (2011). [PubMed: 21764749]
- 8. Komor AC, Kim YB, Packer MS, Zuris JA & Liu DR Programmable editing of a target base in genomic DNA without double-stranded DNA cleavage. Nature 533, 420–4 (2016). [PubMed: 27096365]
- 9. Gaudelli NM et al. Programmable base editing of A•T to G•C in genomic DNA without DNA cleavage. Nature 551, 464–471 (2017). [PubMed: 29160308]
- 10. Anzalone AV et al. Search-and-replace genome editing without double-strand breaks or donor DNA. Nature 576, 149–157 (2019). [PubMed: 31634902]
- 11. Tong Y et al. Highly efficient DSB-free base editing for streptomycetes with CRISPR-BEST. Proc Natl Acad Sci U S A 116, 20366–20375 (2019). [PubMed: 31548381]
- 12. Tong Y, Jørgensen TS, Whitford CM, Weber T & Lee SY A versatile genetic engineering toolkit for *E. coli* based on CRISPR-prime editing. Nat Commun 12, 5206 (2021). [PubMed: 34471126]
- Volke DC, Martino RA, Kozaeva E, Smania AM & Nikel PI Modular (de)construction of complex bacterial phenotypes by CRISPR/nCas9-assisted, multiplex cytidine base-editing. Nat Commun 13, 3026 (2022). [PubMed: 35641501]
- Yuan Q & Gao X Multiplex base- and prime-editing with drive-and-process CRISPR arrays. Nat Commun 13, 2771 (2022). [PubMed: 35589728]
- 15. Aulicino F et al. Highly efficient CRISPR-mediated large DNA docking and multiplexed prime editing using a single baculovirus. Nucleic Acids Res 50, 7783–7799 (2022). [PubMed: 35801912]
- 16. Li H et al. Multiplex precision gene editing by a surrogate prime editor in rice. Mol Plant 15, 1077–1080 (2022). [PubMed: 35619560]
- 17. Gao L et al. Diverse enzymatic activities mediate antiviral immunity in prokaryotes. Science 369, 1077–1084 (2020). [PubMed: 32855333]
- 18. Millman A et al. Bacterial Retrons Function In Anti-Phage Defense. Cell 183, 1551–1561.e12 (2020). [PubMed: 33157039]
- 19. Mestre MR, González-Delgado A, Gutiérrez-Rus LI, Martínez-Abarca F & Toro N Systematic prediction of genes functionally associated with bacterial retrons and classification of the encoded tripartite systems. Nucleic Acids Res 48, 12632–12647 (2020). [PubMed: 33275130]
- Bobonis J et al. Bacterial retrons encode phage-defending tripartite toxin-antitoxin systems. Nature 609, 144–150 (2022). [PubMed: 35850148]
- 21. Yee T, Furuichi T, Inouye S & Inouye M Multicopy single-stranded DNA isolated from a gram-negative bacterium, Myxococcus xanthus. Cell 38, 203–9 (1984). [PubMed: 6088065]
- Inouye S, Hsu MY, Eagle S & Inouye M Reverse transcriptase associated with the biosynthesis
 of the branched RNA-linked msDNA in *Myxococcus xanthus*. Cell 56, 709–17 (1989). [PubMed:
 2465092]
- 23. Lampson BC, Inouye M & Inouye S Reverse transcriptase with concomitant ribonuclease H activity in the cell-free synthesis of branched RNA-linked msDNA of *Myxococcus xanthus*. Cell 56, 701–7 (1989). [PubMed: 2465091]
- 24. Simon AJ, Ellington AD & Finkelstein IJ Retrons and their applications in genome engineering. Nucleic Acids Res 47, 11007–11019 (2019). [PubMed: 31598685]
- 25. Farzadfard F & Lu TK Genomically encoded analog memory with precise in vivo DNA writing in living cell populations. Science 346, 1256272 (2014). [PubMed: 25395541]
- 26. Sharon E et al. Functional Genetic Variants Revealed by Massively Parallel Precise Genome Editing. Cell 175, 544–557.e16 (2018). [PubMed: 30245013]
- 27. Simon AJ, Morrow BR & Ellington AD Retroelement-Based Genome Editing and Evolution. ACS Synth Biol 7, 2600–2611 (2018). [PubMed: 30256621]
- 28. Schubert MG et al. High-throughput functional variant screens via in vivo production of single-stranded DNA. Proc Natl Acad Sci U S A 118, (2021).

29. Lopez SC, Crawford KD, Lear SK, Bhattarai-Kline S & Shipman SL Precise genome editing across kingdoms of life using retron-derived DNA. Nat Chem Biol 18, 199–206 (2022). [PubMed: 34949838]

- 30. Jiang W et al. High-efficiency retron-mediated single-stranded DNA production in plants. Synth Biol (Oxf) 7, ysac025 (2022). [PubMed: 36452068]
- 31. Fishman CB et al. Continuous Multiplexed Phage Genome Editing Using Recombitrons. bioRxiv (2023)
- 32. Mosberg JA, Lajoie MJ & Church GM Lambda red recombineering in *Escherichia coli* occurs through a fully single-stranded intermediate. Genetics 186, 791–9 (2010). [PubMed: 20813883]
- 33. Wannier TM et al. Improved bacterial recombineering by parallelized protein discovery. Proc Natl Acad Sci U S A 117, 13689–13698 (2020). [PubMed: 32467157]
- Palka C, Fishman CB, Bhattarai-Kline S, Myers SA & Shipman SL Retron reverse transcriptase termination and phage defense are dependent on host RNase H1. Nucleic Acids Res 50, 3490– 3504 (2022). [PubMed: 35293583]
- 35. Datsenko KA & Wanner BL One-step inactivation of chromosomal genes in *Escherichia coli* K-12 using PCR products. Proc Natl Acad Sci U S A 97, 6640–5 (2000). [PubMed: 10829079]
- 36. Ellington AJ & Reisch CR Efficient and iterative retron-mediated in vivo recombineering in *Escherichia coli*. Synth Biol (Oxf) 7, ysac007 (2022). [PubMed: 35673614]
- 37. Alper H, Jin YS, Moxley JF & Stephanopoulos G Identifying gene targets for the metabolic engineering of lycopene biosynthesis in *Escherichia coli*. Metab Eng 7, 155–64 (2005). [PubMed: 15885614]
- 38. Kang MJ et al. Identification of genes affecting lycopene accumulation in *Escherichia coli* using a shot-gun method. Biotechnol Bioeng 91, 636–42 (2005). [PubMed: 15898075]
- 39. Jin YS & Stephanopoulos G Multi-dimensional gene target search for improving lycopene biosynthesis in *Escherichia coli*. Metab Eng 9, 337–47 (2007). [PubMed: 17509919]
- 40. Chen H, Bjerknes M, Kumar R & Jay E Determination of the optimal aligned spacing between the Shine-Dalgarno sequence and the translation initiation codon of *Escherichia coli* mRNAs. Nucleic Acids Res 22, 4953–7 (1994). [PubMed: 7528374]
- 41. Engler C, Kandzia R & Marillonnet S A one pot, one step, precision cloning method with high throughput capability. PLoS One 3, e3647 (2008). [PubMed: 18985154]
- 42. Cunningham FXJ, Sun Z, Chamovitz D, Hirschberg J & Gantt E Molecular structure and enzymatic function of lycopene cyclase from the cyanobacterium *Synechococcus* sp strain PCC7942. Plant Cell 6, 1107–21 (1994). [PubMed: 7919981]
- 43. Liu W et al. Retron-mediated multiplex genome editing and continuous evolution in *Escherichia coli*. Nucleic Acids Res 51, 8293–8307, doi:10.1093/nar/gkad607 (2023). [PubMed: 37471041]
- 44. DiCarlo J et al. Genome engineering in *Saccharomyces cerevisiae* using CRISPR-Cas systems. Nucleic Acids Res, 41 (7), 4336–4343 (2013). [PubMed: 23460208]
- 45. DiCarlo J et al. Yeast Oligo-Mediated Genome Engineering (YOGE). ACS Synthetic Biology, 2 (12), 741–749 (2013). [PubMed: 24160921]
- 46. Roy K, et al. Multiplexed precision genome editing with trackable genomic barcodes in yeast. Nat Biotechnol 36, 512–520 (2018). [PubMed: 29734294]
- 47. Guo X, et al. High-throughput creation and functional profiling of DNA sequence variant libraries using CRISPR–Cas9 in yeast. Nat Biotechnol 36, 540–546 (2018). [PubMed: 29786095]
- 48. Świat M et al. *Fn*Cpf1: a novel and efficient genome editing tool for *Saccharomyces cerevisiae*, Nucleic Acids Res, 45 (21), 12585–12598 (2017). [PubMed: 29106617]
- 49. Ferreira R et al. Multiplexed CRISPR/Cas9 Genome Editing and Gene Regulation Using Csy4 in Saccharomyces cerevisiae. ACS Synthetic Biology, 7 (1), 10–15 (2018). [PubMed: 29161506]
- 50. Liang Z et al. Advanced eMAGE for highly efficient combinatorial editing of a stable genome. bioRxiv 2020.08.30.256743.

Methods-Only References:

51. Niwa H, Yamamura K & Miyazaki J Efficient selection for high-expression transfectants with a novel eukaryotic vector. Gene 108, 193–199 (1991). [PubMed: 1660837]

52. Gietz RD & Schiestl RH High-efficiency yeast transformation using the LiAc/SS carrier DNA/PEG method. Nat Protoc 2, 31–4 (2007). [PubMed: 17401334]

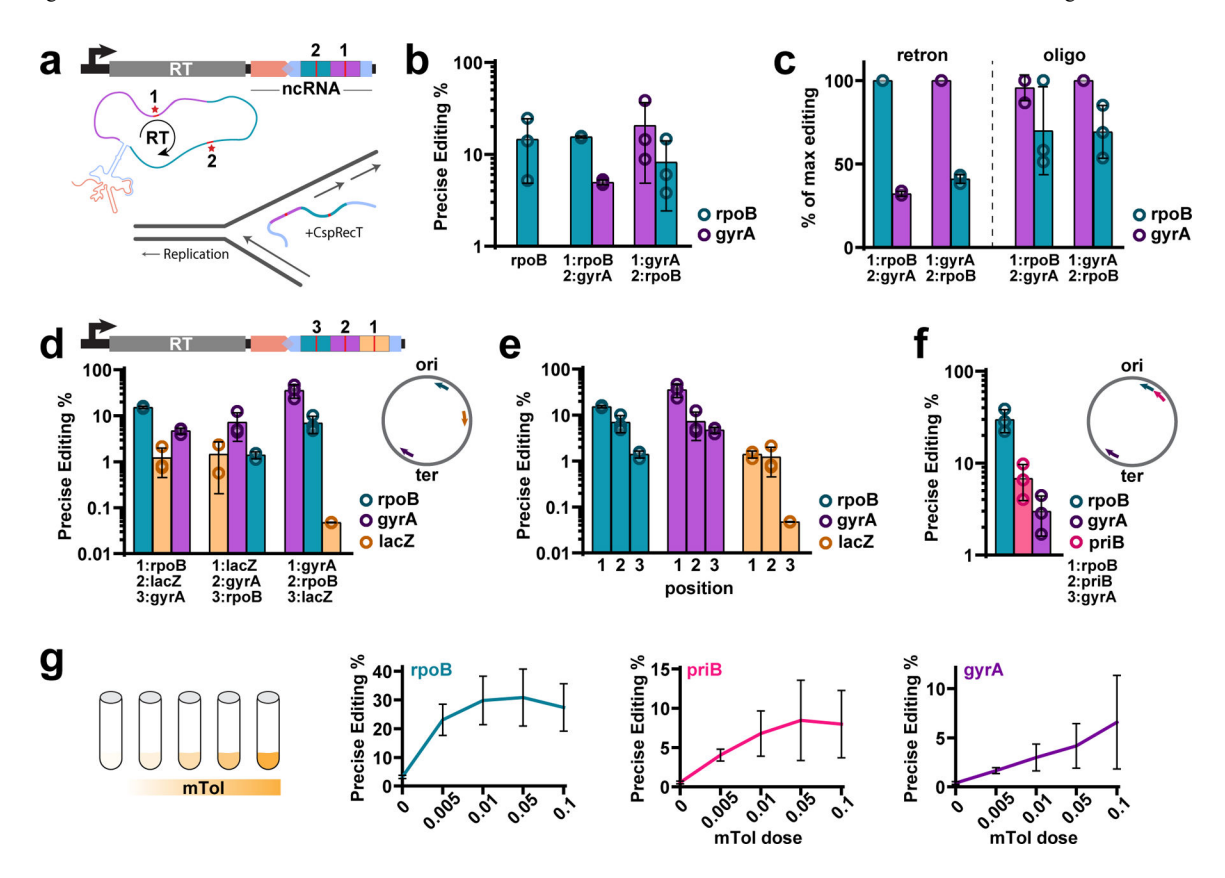


Figure 1.

Encoding several donors in a retron msd enables multiplexed retron recombineering. a. Top: schematic of the retron recombineering operon with two donors encoded within the msd. Donor labels indicate the order in which the donor is reverse transcribed. Bottom: schematic of the retron recombineering process. **b.** Quantification of precise editing rates of the *rpoB* locus alone and both rpoB and gyrA loci in bacteria. The order in which the donors are reverse transcribed is indicated. For b, c, d, e, and f, data were quantified by sequencing after 24h of editing, circles show each of the three biological replicates, bars are mean ±SD (one-way ANOVA, effect of condition on rpoB editing P=0.2616). c. Comparison of donor order for retron-encoded donors versus oligonucleotide donors. Editing is shown as percent of maximum precise editing for each condition. Retron, but not oligonucleotide, is influenced by position effects (one-way ANOVA effect of conditions P<0.0001; Tukey's corrected effect of retron order P < 0.0001, oligo order P = 0.9842). d. Top: schematic of the retron recombineering cassette with 3 donors encoded in the msd. Numbers above indicate order of reverse transcription. Bottom: quantification of precise editing rates of bacterial rpoB, gyrA, and lacZloci. Right: schematic indicating donor position and strand with respect to the origin of replication (lagging strand for rpoB and gyrA donors and leading strand for the lacZ donor). e. Replot of the data in d, illustrating effect of position on editing at each site (two-way ANOVA effect of position P < 0.0001). **f.** Quantification of precise editing rates for rpoB, gyrA and priB, in the architecture shown in d. Right: schematic of donor position and strand respect to the origin of replication. All donors are in the lagging strand (one-way ANOVA, effect of editing site P=0.0015). g. Use of multiplexed retron recombineering to improve analog molecular recording technologies. (left) Increasing

amounts of m-toluic acid (mTol) are recorded using a retron-derived analog recorder; (right) quantification of precise editing rates for rpoB, gyrA and priB loci using different amounts of mTol. Error bars are \pm SD for three biological replicates. Additional statistical details in Supplementary Table 1.

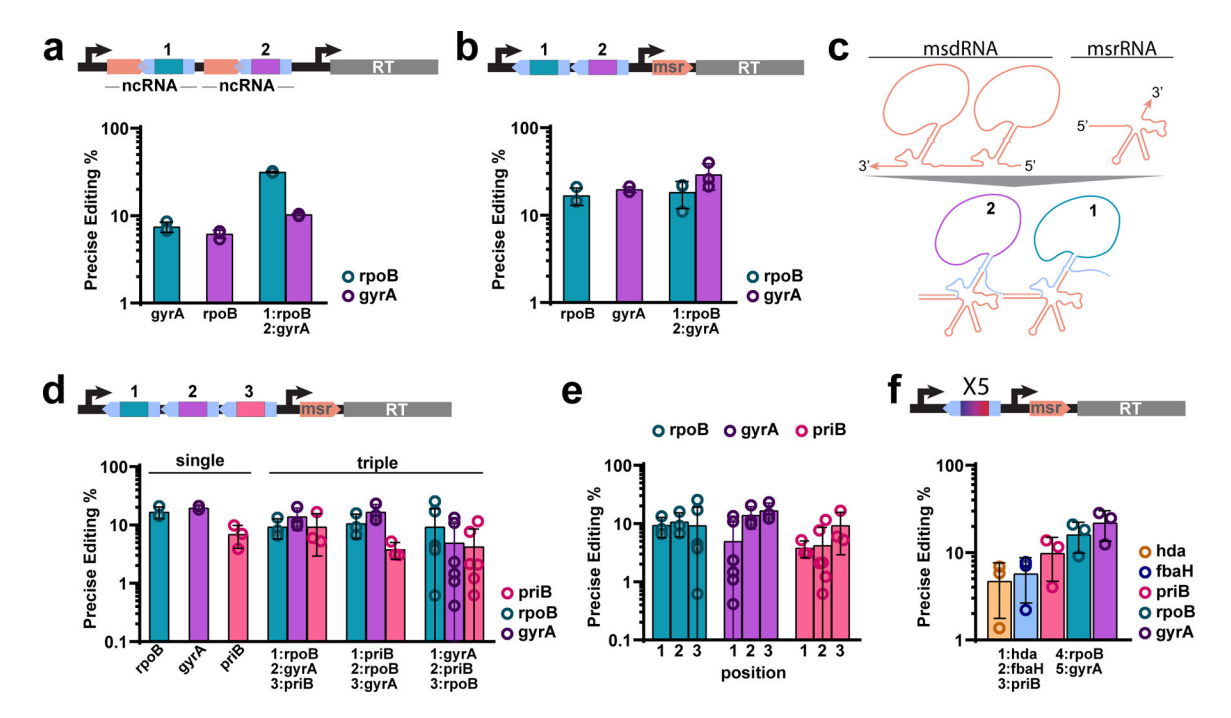


Figure 2. Improved multiplexed editing using donors in arrayed retron msds. a. Top: schematic of retron recombineering using 2 independent ncRNAs. Each msd region (blue) encodes a different donor (1 and 2). Bottom: quantification of precise editing rates for precise editing of gyrA or rpoB alone or simultaneously (unpaired, two-tailed t-test, singleplex versus multiplex, rpoB P<0.0001, gyrA P=0.0006). b. Top: Schematic of retron recombineering using an msd array with a single msr sequence in trans. Bottom: quantification of precise editing rates for precise editing of rpoB or gyrA alone or simultaneously (unpaired, twotailed t-test, singleplex versus multiplex, rpoB P=0.7312, gyrA P=0.1702). c. Top: schematic of arrayed msd and msr transcription products. Arrayed msd is transcribed as a single transcript. Bottom: schematic of RT-DNA production using as template an arrayed msd. 1 and 2 indicates the number of the msd in the arrayed msd. **d.** Top: schematic of 3x arrayed msd. Bottom: quantification of precise editing of rpoB, gyrA or priB edits alone or simultaneously. e. Replot of the data in d, illustrating the effect of position on editing at each site (two-way ANOVA, effect of position P=0.1138). f. Quantification of precise editing using a 5x arrayed msd to edit hda, fbaH, priB, rpoB and gyrA. Data in a, b, d, e and f were quantified by Illumina sequencing after 24h of editing, circles show each of the three biological replicates, bars are mean ±SD (one-way ANOVA effect of editing site P=0.016). Additional statistical details in Supplementary Table 1.

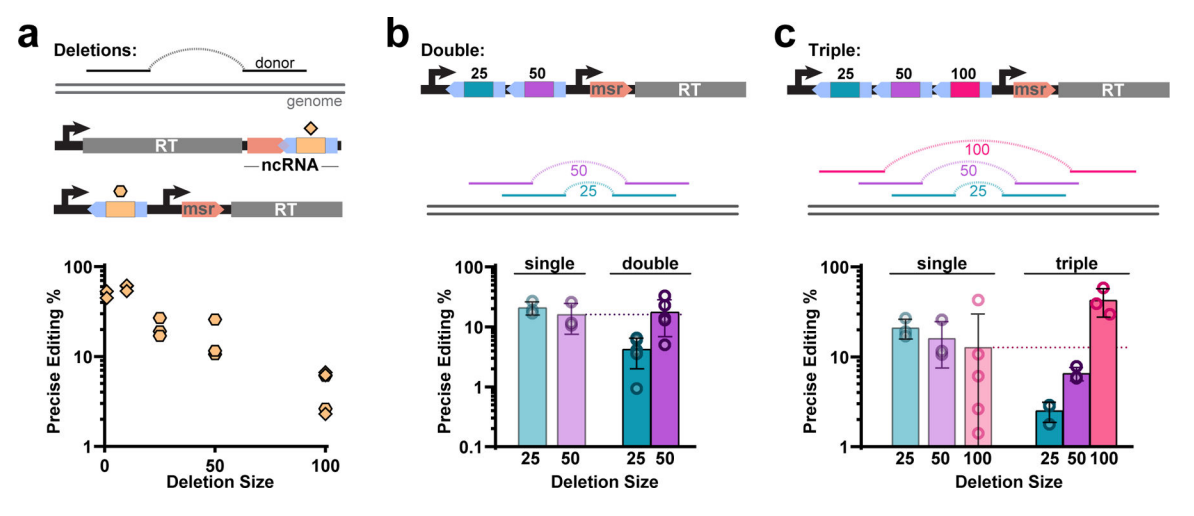


Figure 3.

Increasing limits of deletion size using nested deletion donor arrays. a. Top: Schematic of genome deletions using retron recombineering. Middle: schematic of a standard retron cassette to make deletions (top) with the donor represented by a diamond and an arrayed msd retron cassette with the donor represented by a hexagon. Bottom: quantification of precise editing rates for a single deletion of 1 bp, 10 bp, 25 bp, 50 bp or 100 bp deletions by Illumina sequencing after 24h of editing. Diamonds show deletions from a standard architecture and hexagons show deletions using an arrayed architecture (one-way ANOVA, effect of deletion size P < 0.0001). **b.** Top: Schematic of arrayed msd retron cassette with two donors to make 25 and 50 bp deletions. Middle: Schematic of a nested deletion strategy using two donors to delete 25 bp and 50 bp. If the 25 bp occurs first, the 50 bp deletion becomes a 25 bp deletion. Bottom: Quantification of precise editing rates for single 25 and 50 bp deletions, and for the nested 50 bp deletion (unpaired, two-tailed t-test, 25 base deletion, single vs multi P=0.0006, 50 base deletion, single vs multi P=0.8393).. c. Top: Schematic of arrayed msd retron cassette with three donors to make 25, 50 bp and 100 bp deletions. Middle: Schematic of a nested deletion strategy using three donors to delete 25 bp, 50 bp and 100 bp. Bottom: Quantification of precise editing rates for single 25 bp, 50 bp and 100 bp deletions, and for each deletion using the nested strategy (unpaired, two-tailed t-test, singleplex versus multiplex 100bp deletion, P=0.0485). Data in b and c were quantified by Illumina sequencing 24h after of editing, circles show each of the three biological replicates, bars are mean ±SD. Additional statistical details in Supplementary Table 1.

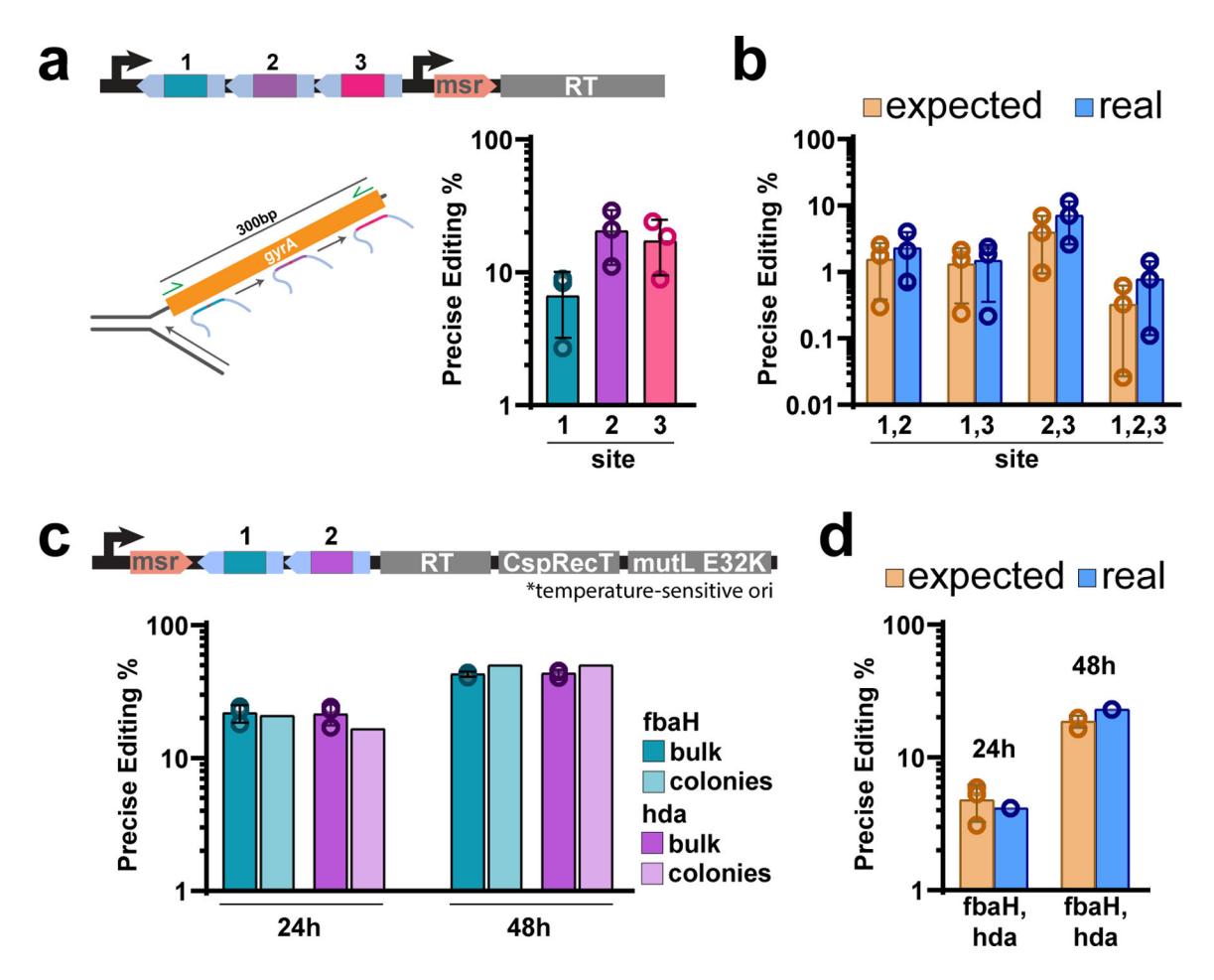


Figure 4. Multisite editing of individual bacterial genomes using multitrons. a. Top: Schematic of retron recombineering using an msd array encoding 3 donors with a single msr sequence in trans. Bottom: (left) schematic of the multitron recombineering process at this locus. All retron donors are able to target the lagging strand of gyrA gene during bacterial replication in a chromosomal window of 300 bp. Green arrows represent the primers used to amplify the target region. (right) quantification of precise editing rates of individual target sites along the gyrA gene, circles show each of the three biological replicates, bars are mean \pm SD. **b.** Quantification of expected (product of bulk rates at each indicated site) and real precise editing rates of double and triple combinatorial edits in the gyrA locus of an individual genome. Circles show each of the three biological replicates, bars are mean ±SD (two-way ANOVA, expected vs real, P=0.0765). c. Top: Schematic of single-plasmid, temperature sensitive multitron architecture. Below: Editing rates for each indicated site at each time point from bulk (Illumina amplicon sequencing) and individual colony sequencing. Circles show each of the three biological replicates, bars are mean ±SD. Mean colony sequencing rates are indicated with a bar. d. Quantification of expected (product of bulk rates at each indicated site) and real precise editing rates of double edits in individual genomes. Circles show each of the three biological replicates, bars are mean ±SD (two-way ANOVA, expected vs real, *P*=0.2734). Colony sequencing represented by a single point.

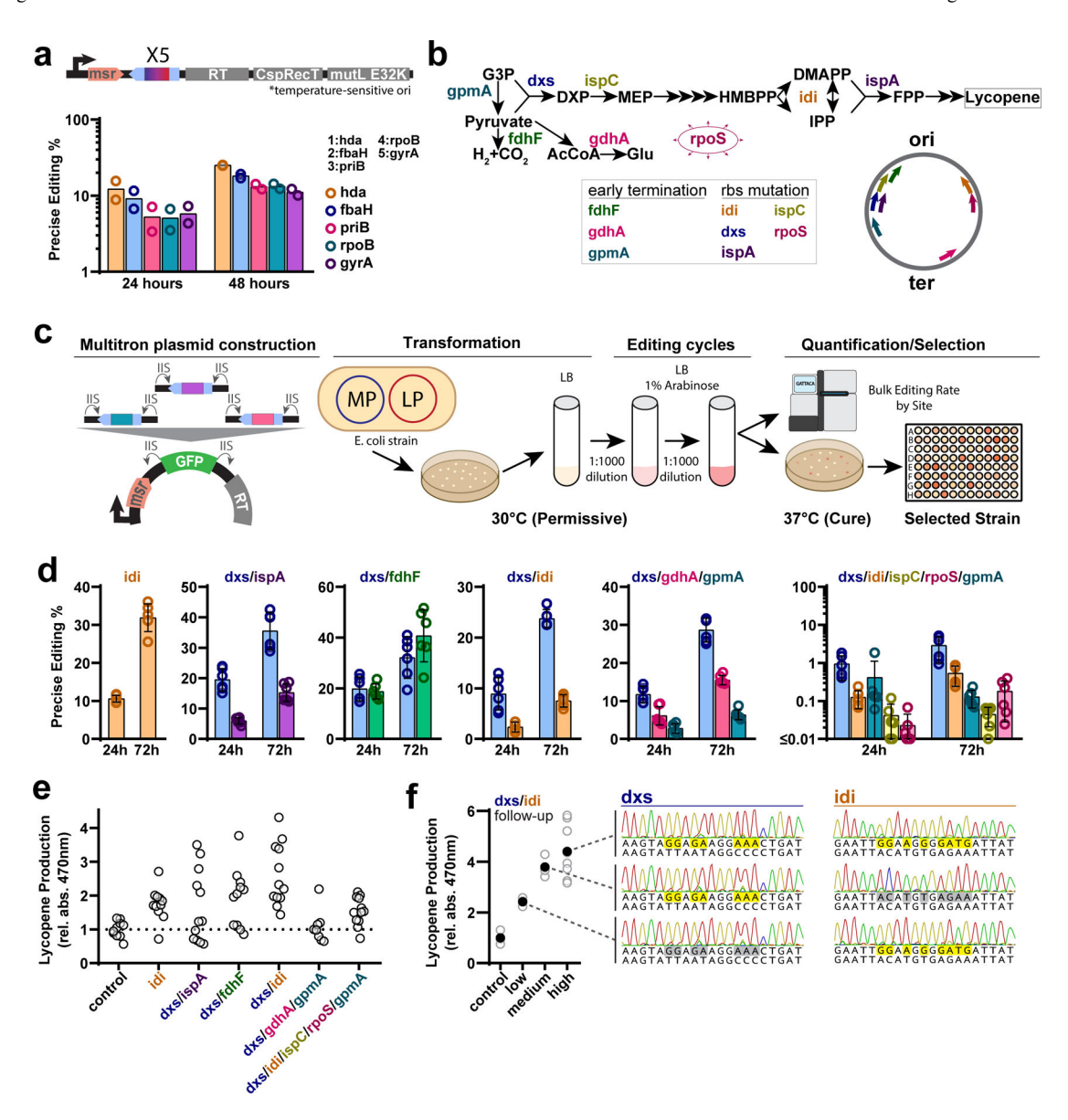


Figure 5.

Metabolic engineering using multitrons. a. Top: architecture of the multiplexed retron recombineering cassette in the temperature sensitive plasmid. The operon is composed of a single msr followed by 5x arrayed msds with donors and the genes encoding the RT, the CspRecT and the dominant negative MutLE32K. Bottom: quantification of precise editing rates using a 5x arrayed msd to edit hda, fbaH, priB, rpoB and gyrA by Illumina sequencing 24h and 48h after of editing (two-way ANOVA, effect of expression time P<0.0001). Circles show each of the three biological replicates, bars are mean ±SD. The order of the donors in the arrayed msd is indicated. b. Top: Schematic of the lycopene biosynthesis pathway, with key genes to increase lycopene production highlighted. Bottom: Schematic of metabolic engineering of lycopene biosynthesis pathway using multiplexed retron recombineering. c. The donors are cloned into a temperature sensitive backbone using a golden gate assembly protocol. Single colonies are grown for 24 h and then induced with arabinose. This cycle

is repeated by making 1:1000 dilutions for several days. Editing rates are measured by Illumina sequencing and cultures are plated to select individual colonies based on color for quantification of lycopene production. **d.** Quantification of precise editing rates using different recombitron plasmids containing a variable number of donors to edit genes in the lycopene pathway, quantified by Illumina sequencing after 24h and 72h. Circles show each of the six biological replicates, bars are mean ±SD. **e.** Quantification of lycopene production in single colonies. Lycopene production was normalized against the average production of the control, which contains the pAC-LYC but was not exposed to the recombineering process. Each point represents a colony (n=12). **f.** Quantification of lycopene production from colonies re-isolated from samples in the low (~2X control), medium (~3X control), and high (~4x control) production clusters of the *dxs/idi* condition. Open circles are individual colony values (3 biological replicates or the control, low, and medium groups; eight biological replicates for the high group) and closed circles are the mean. Sanger sequencing examples to the right illustrate the genotype of each subset (all individual colonies within a condition have identical genotypes). Additional statistical details in Supplementary Table 1.

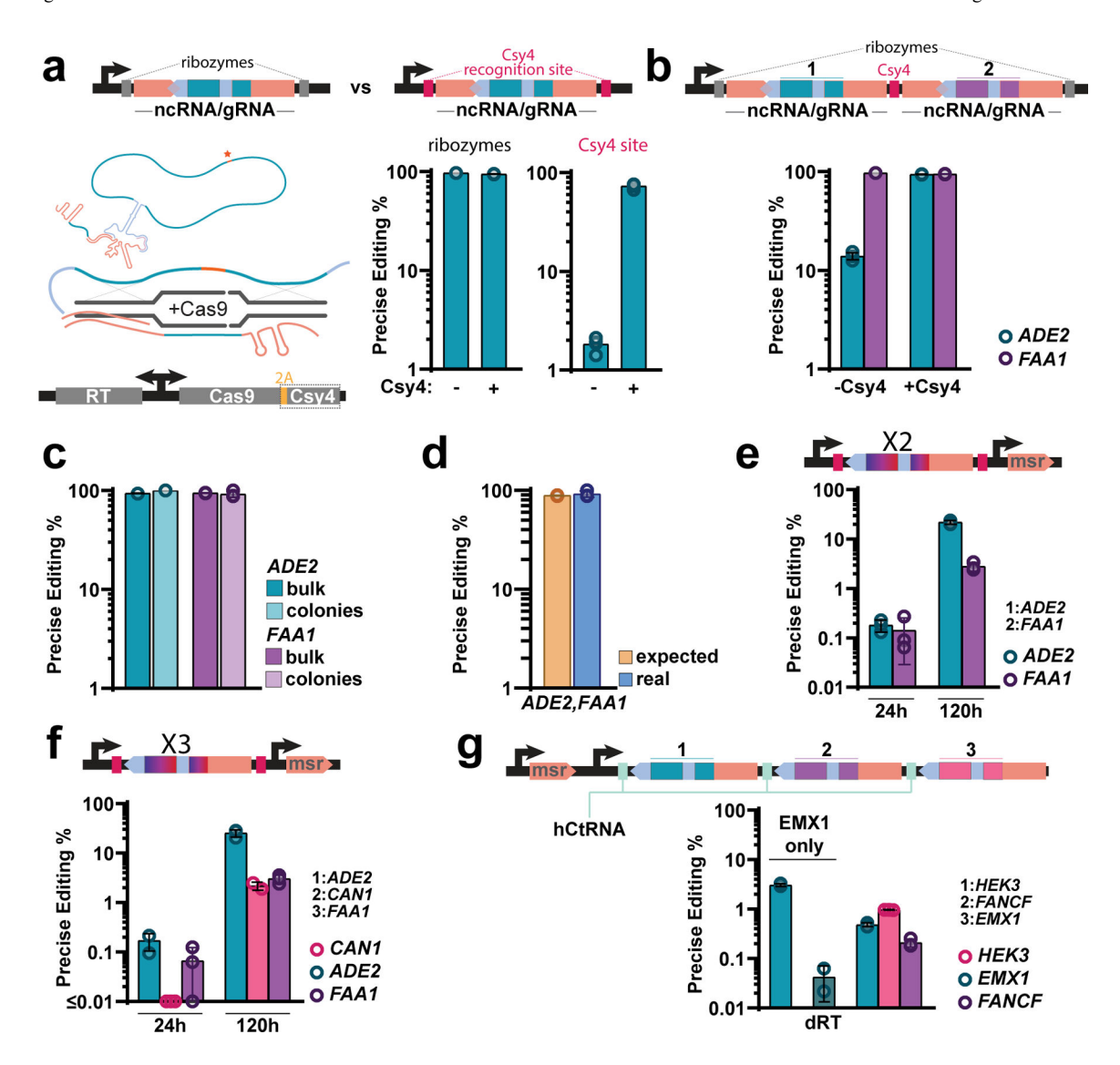


Figure 6. Arraved

Arrayed retron msds enable multiplexed editing in eukaryotic cells. **a-g**: quantification of precise editing was determined by Illumina sequencing after 48h (yeast) and 72h (HEK293T), unless specified; circles show each of the three biological replicates, bars are mean ±SD. **a.** Top: schematic of the donor-encoding retron ncRNA/gRNA cassette, expressed from a Gal7 promoter and flanked by ribozymes or Csy4 sequences. Bottom left: schematic of a retron ncRNA/gRNA hybrid, depicted above the yeast genome-encoded protein-coding expression cassette. Bottom right: quantification of precise editing of the yeast *ADE2* locus. Absence/presence of Csy4 in the protein-coding expression cassette is shown below the graph (Sidak's corrected multiple comparisons, effect of Csy4 expression, ribozyme construction *P*=0.2779, Csy4 construct *P*<0.0001). **b.** Top: schematic of an arrayed retron ncRNA/gRNA cassette, expressed from a Gal7 promoter, flanked by ribozymes, and separated by a Csy4 sequence. The editors in positions 1 and 2 target the *ADE2* and *FAA1* loci, respectively. Bottom: quantification of precise editing of the yeast *ADE2* and *FAA1* loci. Absence/presence of Csy4 in the protein-coding expression cassette is shown

below the graph (Sidak's corrected multiple comparisons, effect of csy4 expression, ADE2 P<0.0001, FAA1 P=0.0012). **c.** Editing rates for each locus and time point from bulk and individual colony sequencing (bar represents mean). **d.** Quantification of expected (product of bulk rates) and real precise editing rates of double edits in individual genomes (two-way ANOVA, expected vs real, P=0. 0.4318). **e-f**, top: schematic of 2- and 3x arrayed retron msdRNA-gRNA cassettes, as shown in Extended Data Fig. 4c. Bottom: quantification of precise editing of the yeast ADE2 and FAA1 (e); and ADE2, CAN1 and FAA1 (f) loci, after 24 and 120h of editing. Two-way ANOVA, effect of expression time, e P<0.0001, f P<0.0001. **g.** Arrayed retron msds enable multiplexed editing in human cells. Top: schematic of the donor-encoding retron ncRNA/gRNA expression cassette expressed from an H1 promoter and flanked by tRNA-Cys-GCA (hCtRNA) sequences. Bottom: quantification of precise editing of the HEK293T EMX1, HEK3 and FANCF loci. Absence/presence of a catalytically active retron RT is shown below the graph. Additional statistical details in Supplementary Table 1.